Journal of Mathematical Modeling
Vol. -, No. -, 2026, pp. -. Research Article

JMM

Solution of time fractional Black-Scholes PDE using fractional order generalized Chelyshkov wavelets

Sufia Sabir*, **Ayaz Ahmad**

Department of Mathematics and Computing Technology, National Institute of Technology Patna, Patna, 800005, Bihar, India

Email(s): sufias.phd22.ma@nitp.ac.in, ayaz@nitp.ac.in

Abstract. This paper presents an efficient numerical technique for solving the time-fractional Black-Scholes equation, which models the pricing of European options. The proposed method is based on a fractional order generalized Chelyshkov wavelets (FOGCW), a generalized form of classical wavelets. The computation of the Riemann-Liouville fractional integral operator (RLFIO) is a key point of this method. An exact formulation of RLFIO corresponding to FOGCW is obtained. The RLFIO of the traditional Chelyshkov wavelet has been previously obtained through Laplace transform techniques; however, due to the complex structure of the scaling and modulation parameters of generalized fractional order, this technique does not work. In this work, we have utilized the regularized beta function to derive an exact formula for the RLFIO of FOGCW. Several numerical examples are presented to confirm the accuracy and efficiency of the proposed method. Error analysis is also conducted.

Keywords: Time fractional Black-Scholes equation, fractional order generalized Chelyshkov wavelet, regularized beta function, error analysis.
AMS Subject Classification 2010: 35A01, 65L10, 65L12, 65L20, 65L70.

1 Introduction

An option is a contractual instrument that provides its holder the right, but not an obligation, to buy or sell an underlying asset at a fixed strike price on or before a certain date. European options are a fundamental type of option that can be exercised only at the time of their expiration. Black-Scholes equation (BSE) is a mathematical model introduced in 1973 by Black, Scholes, and Merton, to determine the price of an European options [1]. The BSE is a parabolic partial differential equation and plays an important role in modern option pricing theory. Traditional BSE is based on integer-order derivatives that fail to accurately

*Corresponding author
Received: 05 December 2025/ Revised: 28 April 2026/ Accepted: 30 April 2026
DOI: 10.22124/jmm.2026.32461.2944

capture the non-local and complex behavior of stock prices observed in practice. It is built on the assumptions of market efficiency, short memory, and Markovian price dynamics. These assumptions imply that the asset returns follow a memoryless stochastic process driven by standard Brownian motion. However, extensive studies on financial markets have consistently reported the deviations from these assumptions, including the presence of long-range dependence, persistence behavior, and volatility in asset return and associated financial variables. Such empirical evidence shows the influence of historical information on the dynamics of financial markets. Fractional calculus has emerged as an important mathematical tool that deals with systems that exhibit non-local behavior and memory-dependent dynamics. Its application can be seen in various domains of science and engineering [2, 3]. Their wide applicability has made fractional differential equations a subject of growing interest in recent years [4, 39, 40]. In contrast to the classical integer-order derivatives, fractional derivatives remember past information of the system, making them suitable for modeling financial markets where long-memory effects are present. Motivated by these aspects, this paper presents a fractional-order Black-Scholes model to capture asset price dynamics [5, 6] more accurately. Wyss et al. [7] proposed the time fractional Black-Scholes equation (TFBSE) for European options. Cartea and Del Castillo-Negretta [8] studied a one-dimensional space fractional model. Liang et al. [9] presented a time-fractional Black-Scholes Merton equation, which was improved by Chen et al. [10]. The exact solution of TFBSE may not be possible in many cases. Therefore, numerical schemes were used to find solutions of various kinds of TFBSE. She et al. [11] applied the Adomian decomposition method to find the solution of TFBSE. The generalized Laplace homotopy perturbation method is used by Ampun and Sawangtong [12] to solve TFBSE. Kazami [13] presented a second-order numerical scheme to solve TFBSE for European option pricing. Roul and Goura [14] applied a finite difference scheme for the TFBSE. [15] used Jacobi polynomials to solve TFBSE.

Recently, wavelet-based methods have been employed to solve various types of fractional partial differential equations (FPDE). A wavelet is a function that is obtained by scaling and translation of a basis function called a mother wavelet. Wavelet has several inherent properties like excellent localization, multi-resolution characteristics, and compactly supported basis, which provide accuracy and stability to the numerical scheme. Furthermore, wavelets can capture the singularities in fractional models very effectively. Haar wavelet [16], Bernoulli wavelet [17], Chebyshev wavelet [18], Legendre wavelet [19] are some commonly known wavelets that are used to solve time fractional partial differential equations (TFPDE). Later, fractional order wavelets [20] are introduced to increase the accuracy of the method. In these methods, fractional derivatives and integrals are approximated using operational matrices. However, since the approximation techniques are used in the construction of these matrices, the computed fractional derivatives and integrals include errors, which may increase the total computational error. To tackle this situation, authors in [21, 22] used the Laplace transform to compute an exact formulation of the Riemann-Liouville fractional integral operator (RLFIO), which eliminates the need for operational matrices. But due to the complex structure involved in fractional order wavelets, this method cannot be directly extended.

The novelties of the proposed work are given as follows:

1. The statistical justification for the fractional framework by examining the memory properties of financial time series is discussed.
2. A novel fractional-order generalized Chelyshkov wavelets (FOGCW) for solving the fractional Black-Scholes model is introduced.
3. The concept of the regularized beta function (a special type of hypergeometric function) is used to find an exact formula for the RLFIO of FOGCW, which removes the error obtained by using several

approximation techniques during the calculation of RLFIO.
4. A detailed analysis of the error bound is presented.
5. Several numerical examples are taken to show the effectiveness of the proposed method. A detailed comparison of proposed method with the other existing methods [23–33] is done.

The rest of the article is organized as follows: Section 1 presents the introduction part. Section 2 presents the memory property analysis of the financial market. Section 3 presents the model description. Section 4 presents mathematical preliminaries and the development of the fractional order generalized Chelyshkov wavelets. Error analysis is done in Section 5. Numerical examples are provided in Section 6. The conclusion of the article is presented in Section 7.

2 Memory property analysis of financial market

Classical Black Scholes model, given by Fischer Black and Myron Scholes, assumes that the asset returns follow a Markov process with independent increments. However, empirical evidence shows that the financial time series exhibit long-range dependence and volatility persistence, indicating the presence of memory effects. To show the presence of memory in financial markets, we have taken daily closing price data for two major United States equity market indices, the S&P 500 and the NASDAQ composite. A broad segment of the United States financial market is represented by these two indices, with the S&P 500 reflecting large capitalization stocks and the NASDAQ composite being dominated by technology oriented firms. The sample period spans from Jan 2016 to Dec 2025, and covers different market regimes, including pre-crisis, crisis, and post-crisis period. To evaluate the memory properties of the financial markets, we use the Rescaled range analysis, a widely used method for estimating the Hurst exponent (H). The quantitative value of the Hurst exponent helps to examine long memory. First, we transform the daily closing prices into logarithmic returns to ensure stationarity and comparability across time. The return series is obtained as the first difference of the natural logarithm of consecutive prices. Rescaled range analysis, which estimates the Hurst exponent by examining the scaling behavior of cumulative deviations from the mean across multiple time scales. Specifically, first, we divide the return series into non-overlapping subseries, and the rescaled range is obtained by taking the ratio of the range of cumulative deviations to the corresponding standard deviation. Then, we obtain a log-log regression between the average rescaled range and the time scale; the slope of this regression provides the estimate of the Hurst exponent. The H can be classified into distinct cases. When H=0.5, the series behaves as a purely random. If $0 < H < 0.5$, the series exhibits mean-reverting behavior. If $0.5 < H < 1$, it shows the presence of long memory, implying a clear trend structure in which an increase or decrease in the subsequent period depends on the increase or decrease in the previous period. Table 2 shows the long memory estimates for the return series of the S&P 500 and NASDAQ composite indices over the full sample period. The results show that the long memory is present in the returns of both indices. Table 3 presents the long memory estimates for the pre-crisis, crisis, and post-crisis period. In all three periods, long memory is present in both indices. Table 4 presents the long memory estimate of individual years for S&P 500 and NASDAQ. The estimated Hurst exponents for both indices consistently exceed 0.5 across each year except one year, which is 2017, in which NASDAQ shows the absence of memory.

The empirical analysis done in this section confirms the presence of long-range dependence in the financial return series. The estimated Hurst exponent exceeding 0.5 indicates persistent memory effects

Table 1: Data description

Index	No. of observations	Period cover
S&P 500	2607	2016–2025
NASDAQ	2607	2016–2025

Table 2: Hurst exponent for full period

Period	Index	Hurst Exponent	Memory property
2016–2025	S&P 500	0.5531	Long memory is present
	NASDAQ	0.5536	Long memory is present

Table 3: Pre-Crisis, Crisis and Post-Crisis

Period	Index	Hurst Exponent	Memory property
2016–2019	S&P 500	0.5794	Long memory is present
	NASDAQ	0.5487	Long memory is present
2020–2021	S&P 500	0.5322	Long memory is present
	NASDAQ	0.5659	Long memory is present
2022–2025	S&P 500	0.5719	Long memory is present
	NASDAQ	0.5690	Long memory is present

Table 4: Hurst exponent for each year

Period	Index	Hurst Exponent	Memory property
2016	S&P 500	0.6242	Long memory is present
	NASDAQ	0.6481	Long memory is present
2017	S&P 500	0.5242	Long memory is present
	NASDAQ	0.4897	Long memory is absent
2018	S&P 500	0.6119	Long memory is present
	NASDAQ	0.6186	Long memory is present
2019	S&P 500	0.5879	Long memory is present
	NASDAQ	0.5801	Long memory is present
2020	S&P 500	0.6273	Long memory is present
	NASDAQ	0.5415	Long memory is present
2021	S&P 500	0.5105	Long memory is present
	NASDAQ	0.5921	Long memory is present
2022	S&P 500	0.5953	Long memory is present
	NASDAQ	0.5637	Long memory is present
2023	S&P 500	0.6324	Long memory is present
	NASDAQ	0.6596	Long memory is present
2024	S&P 500	0.575	Long memory is present
	NASDAQ	0.5821	Long memory is present
2025	S&P 500	0.5221	Long memory is present
	NASDAQ	0.5317	Long memory is present

in market dynamics. Such behavior contradicts the assumptions of the classical Black-Scholes model, which involves a local first-order time derivative and cannot capture the historical information of the pricing mechanism. While fractional derivatives are non-local operators that contain the entire past history information of the process. Therefore, the adoption of a time-fractional Black-Scholes model which contain memory effects provides a consistent mathematical framework for modeling financial markets.

3 Time fractional Black-Scholes model

Motivated by the analysis of Section 2, in this section, we consider the TFBSE with initial and boundary conditions as follows from [34]:

$$ {}^{C}D_{\tau}^{\beta}u(x,\tau)+\frac{1}{2}\sigma^2x^2\frac{\partial^2u(x,\tau)}{\partial x^2}+rx\frac{\partial u(x,\tau)}{\partial x}-ru(x,\tau)=0,\quad (x,\tau)\in\mathbb{R}^+\times(0,T], \tag{1}$$

with I.C and B.Cs

$$ u(x,0)=\chi(x),\qquad u(0,\tau)=p(\tau),\qquad u(\infty,\tau)=q(\tau), \tag{2}$$

where $0<\beta\leq 1$, r denotes the risk-free interest rate, x is the stock price, τ is the maturity time, σ is the volatility of the returns, u is the price of a European option, and

$$ {}^{C}D_{\tau}^{\beta}u(x,\tau)=\begin{cases}\dfrac{1}{\Gamma(1-\beta)}\dfrac{d}{d\tau}\displaystyle\int_{\tau}^{T}\frac{u(x,\xi)-u(x,T)}{(\xi-\tau)^{\beta}}d\xi, & 0<\beta<1,\\[2ex] \dfrac{\partial u(x,\tau)}{\partial\tau}, & \beta=1.\end{cases} \tag{3}$$

Substituting $\tau=T-t$, Equation (3) converts into

$$\begin{aligned} {}^{C}D_{\tau}^{\beta}u(x,\tau)&=\frac{1}{\Gamma(1-\beta)}\frac{d}{d\tau}\int_{\tau}^{T}\frac{u(x,\xi)-u(x,T)}{(\xi-\tau)^{\beta}}d\xi,\\ &=-\frac{1}{\Gamma(1-\beta)}\frac{d}{dt}\left(\int_{T-t}^{T}\frac{u(x,\xi)-u(x,T)}{(\xi-(T-t))^{\beta}}d\xi\right),\\ &=-\frac{1}{\Gamma(1-\beta)}\frac{d}{dt}\left(\int_{0}^{t}\frac{u(x,T-t)-u(x,T)}{(t-\eta)^{\beta}}d\eta\right). \end{aligned}$$

Let $x=\ln s$. Then model (1) can be written as

$$\begin{cases} {}^{C}D_{t}^{\beta}\mathscr{U}(s,t)=\dfrac{1}{2}\sigma^2\dfrac{\partial^2\mathscr{U}(s,t)}{\partial s^2}+(r-\frac{1}{2}\sigma^2)\dfrac{\partial\mathscr{U}(s,t)}{\partial s}-r\mathscr{U}(s,t),\\ \mathscr{U}(s,0)=\rho(s),\\ \mathscr{U}(s,\tau)=p(t)\quad \text{as } s\to-\infty,\\ \mathscr{U}(s,\tau)=q(t)\quad \text{as } s\to\infty, \end{cases}$$

where

$$ {}^{C}D_t^{\beta}\mathscr{U}(s,t) = \frac{1}{\Gamma(1-\beta)}\frac{d}{dt}\int_0^t \frac{\mathscr{U}(s,\eta)-\mathscr{U}(s,0)}{(t-\eta)^{\beta}}\,d\eta. \tag{4} $$

To find the approximate solution, we truncate the domain $\mathbb{R}^+ \times (0,T]$ to the finite domain $\mathscr{H} = S \times G$, where $S = (L,R)$ and $G = (0,T]$. We consider the following problem:

$$ \begin{cases} {}^{C}D_t^{\beta}\mathscr{U}(s,t) = \mathscr{P}\dfrac{\partial^2\mathscr{U}(s,t)}{\partial s^2} + \mathscr{Q}\dfrac{\partial\mathscr{U}(s,t)}{\partial s} - \mathscr{R}\mathscr{U}(s,t) + \mathscr{F}(s,t), & (s,t)\in\mathscr{H}, \\ \mathscr{U}(s,0) = \rho(s), & s\in\overline{S}, \\ \mathscr{U}(L,t) = p(t), \quad \mathscr{U}(R,t) = q(t), & t\in\overline{G}, \end{cases} \tag{5} $$

where

$$ \mathscr{P} = \sigma^2/2\ (>0), \qquad \mathscr{Q} = r - \mathscr{P}, \qquad \mathscr{R} = r\ (>0), $$

and $\mathscr{F}(s,t)$ denotes the source term.

4 Mathematical preliminaries and development of the fractional order generalized Chelyshkov wavelets

This section presents the mathematical foundation and the construction of the proposed fractional order generalized Chelyshkov wavelets method. We first discuss the essential concept of fractional calculus required for the formulation of the proposed problem. Subsequently, the fractional order generalized Chelyshkov wavelet basis is introduced, and the approximation properties of functions are discussed. The motivation behind adopting the FOGCW lies in its orthogonality, compact support, and computational efficiency, which make it suitable for handling FPDE. By using the concept of exact formulation of RLFIO of FOGCW, the proposed fractional problem is transformed into a system of algebraic equations, which significantly reduces computational complexity.

Definition 1 ([35]). *A real function $u(s)$, $s>0$, is said to be in the space C_ζ, $\zeta\in R$, if there is a real number $\eta\,(\eta>\zeta)$ such that $u(s) = s^{\eta}u_0(s)$, where $u_0(s)\in C[0,\infty)$ and $u(s)\in C_\zeta^n$ if $u^n(s)\in C_\zeta, \zeta\in\mathbb{N}$.*

Definition 2 ([35]). *The Riemann-Liouville integral I^{β} for a function $u(s)\in C_\lambda$, where $\lambda\geq -1$ is given by*

$$ I^{\beta}u(s) = \begin{cases} \dfrac{1}{\Gamma(\beta)}\displaystyle\int_0^s (s-w)^{\beta-1}u(w)dw, & \beta>0, \\ u(s), & \beta=0, \end{cases} $$

where $\Gamma(.)$ denotes the Gamma function.

Definition 3 ([35]). *The Caputo fractional derivative ${}^{C}D_t^{\beta}$ for a function $u(s)\in C_1^n$ is given by*

$$ {}^{C}D_t^{\beta}u(s) = \begin{cases} \dfrac{1}{\Gamma(n-\beta)}\displaystyle\int_0^s \frac{u^n(w)}{(s-w)^{\beta+1-n}}dw, & n-1<\beta<n, \\ u^n(s), & \beta=n\in\mathbb{N}. \end{cases} $$

The properties of the fractional derivative operator are defined below:

- ${}^{C}D_t^{\beta} I^{\beta} u(s) = u(s)$,
- ${}^{C}D_t^{\gamma} I^{\beta} u(s) = I^{\beta-\gamma} u(s)$, $\beta > \gamma$,
- $I^{\beta}\,{}^{C}D_t^{\beta} u(s) = u(s) - \sum_{k=0}^{n-1} u^{k}(0^{+})\frac{s^{k}}{k!}$, $n-1 < \beta < n$,
- ${}^{C}D_t^{\beta} s^{m} = \begin{cases} 0, & m \in N_0,\ m < \beta, \\ \frac{\Gamma(m+1)}{\Gamma(m+1-\beta)} s^{m-\beta}, & \textit{otherwise.} \end{cases}$

Definition 4 ([36]). *The regularized beta function is defined as*

$$\mathscr{I}(s;p,q) = \frac{\Gamma(p+q)}{\Gamma(p)\Gamma(q)} \int_0^s w^{p-1}(1-w)^{q-1} dw. \tag{6}$$

The next lemma deals with the formulation of RLFIO of $s^{\alpha}\mu_d(s)$ which is used in the exact formula of RLFIO for FOGCW.

Lemma 1 ([36]). *Let $d \geq 0$. For $\alpha \geq -1$*

$$I^{\beta}(s^{\alpha}\mu_d(s)) = \frac{\Gamma(1+\alpha)s^{\alpha+\beta}}{\Gamma(1+\alpha+\beta)} \left[1 - \mathscr{I}\left(\frac{d}{s}; 1+\alpha, \beta\right)\right] \mu_d(s), \tag{7}$$

where

$$\mu_d(s) = \begin{cases} 1, & s \geq d, \\ 0, & \textit{otherwise}. \end{cases}$$

4.1 Fractional order generalized Chelyshkov wavelets and function approximation

Fractional order Chelyshkov wavelets are a class of wavelet functions constructed from Chelyshkov polynomials and extended through fractional order calculus. These wavelets are particularly suited in signal processing, finance, and approximation theory by offering an efficient tool for the representation and analysis of functions and signals. The primary motivation for introducing fractional order generalized Chelyshkov wavelets lies in the need for a flexible, accurate, and computationally efficient numerical framework for solving fractional-order problems. The FOGCW enhance numerical stability because of the orthogonal basis set. It exhibits a high rate of convergence, requiring fewer basis functions to achieve high accuracy in numerical solutions for fractional order problems.

The Chelyshkov wavelets on $[0,1)$ are given as

$$\psi_{n,m}(t) = \begin{cases} 2^{\frac{k-1}{2}}\sqrt{2m+1}\,\mathscr{P}_{m,M}(2^{k-1}t - n + 1), & \frac{n-1}{2^{k-1}} \leq t < \frac{n}{2^{k-1}}, \\ 0, & \text{otherwise.} \end{cases} \tag{8}$$

Putting $t = (\frac{s}{h})^{\alpha}$ in Equation (8), FOGCW on $[0,h)$ are given as [36]:

$$\psi_{n,m}^{h,\alpha}(s) = \begin{cases} 2^{\frac{k-1}{2}}\sqrt{2m+1}\,\mathscr{P}_{m,M}\left(\dfrac{2^{k-1}s^{\alpha}}{h^{\alpha}} - n + 1\right), & h\left(\frac{n-1}{2^{k-1}}\right)^{\frac{1}{\alpha}} \leq s < h\left(\frac{n}{2^{k-1}}\right)^{\frac{1}{\alpha}}, \\ 0, & \text{otherwise,} \end{cases} \tag{9}$$

where h and $\alpha \in \mathbb{R}^+$, k and $M \in \mathbb{Z}^+, n = 1, \ldots, 2^{k-1}$, and $\mathscr{P}_{m,M}(s)$ denotes the Chelyshkov polynomials given as

$$\mathscr{P}_{m,M}(s) = \sum_{j=0}^{M-m-1} c_{j,m} s^{m+j}, m = 0, 1, \ldots M-1, \tag{10}$$

where $c_{j,m} = (-1)^j \binom{M-1-m}{j} \binom{M+m+j}{M-1-m}$.
In two dimensions, FOGCW can be defined as

$$\psi^{\alpha_1,\alpha_2}_{n_1,m_1,n_2,m_2}(s,t) = \begin{cases} 2^{\frac{k_1-1}{2}} 2^{\frac{k_2-1}{2}} \sqrt{2m_1+1}\sqrt{2m_2+1} \\ \mathscr{P}_{m_1,M_1}\left(\frac{2^{k_1-1}s^{\alpha_1}}{h_1^{\alpha_1}} - n_1 + 1\right) \mathscr{P}_{m_2,M_2}\left(\frac{2^{k_2-1}t^{\alpha_2}}{h_2^{\alpha_2}} - n_2 + 1\right), \\ \qquad h_1\left(\frac{n_1-1}{2^{k_1-1}}\right)^{\frac{1}{\alpha_1}} \le s < h_1\left(\frac{n_1}{2^{k_1-1}}\right)^{\frac{1}{\alpha_1}}, \\ \qquad h_2\left(\frac{n_2-1}{2^{k_2-1}}\right)^{\frac{1}{\alpha_2}} \le t < h_2\left(\frac{n_2}{2^{k_2-1}}\right)^{\frac{1}{\alpha_2}}, \\ 0, \qquad \text{otherwise}, \end{cases}$$

where $n_1, m_1, n_2, m_2, k_1, k_2, h_1, h_2$ have their usual meaning, $\mathscr{P}_{m_1,M_1}$, $\mathscr{P}_{m_2,M_2}$ are Chelyshkov polynomials defined in Equation (10) and $\psi^{\alpha_1,\alpha_2}_{n_1,m_1,n_2,m_2}(s,t)$ forms a basis for $L^2([0,h_1) \times [0,h_2))$.
The orthonormality of Chelyshkov wavelets forms the theoretical basis of the proposed method, as it provides independence of the basis functions. The next lemma presents the orthonormality property proved in [36], and used in the subsequent development of the proposed method.

Lemma 2. *The FOGCW are orthonormal on* $[0,h)$ *with respect to weight function* $\mathscr{W}_\alpha(t) = \frac{\alpha t^{\alpha-1}}{h^\alpha}$.

Proof. The proof follows from [36]. □

The next lemma deals with the orthonormality property of FOGCW in two dimensions, case. The result of Lemma 2 is used to prove this lemma. It enables efficient computation of the expansion coefficient.

Lemma 3. *In two dimensions,* $\psi^{\alpha_1,\alpha_2}_{n_1,m_1,n_2,m_2}(s,t)$ *are orthonormal on* $[0,h_1) \times [0,h_2)$ *with respect to the weight function* $\mathscr{W}_{\alpha_1,\alpha_2}(s,t) = \frac{\alpha_1\alpha_2 s^{\alpha_1-1}t^{\alpha_2-1}}{h_1^{\alpha_1}h_2^{\alpha_2}}$.

Proof. Using orthonormal property of FOGCW, we have

$$\int_0^h \mathscr{W}_{\alpha_1}(t)\psi^{h,\alpha_1}_{n_1,m_1}(t)\psi^{h,\alpha_1}_{n_2,m_2}(t)dt = \delta_{n_1n_2}\delta_{m_1m_2}. \tag{11}$$

Now

$$\begin{aligned} &\int_0^{h_1}\int_0^{h_2} \mathscr{W}_{\alpha_1,\alpha_2}(s,t)\psi^{\alpha_1,\alpha_2}_{n_1,m_1,n_2,m_2}(s,t)\psi^{\alpha_1,\alpha_2}_{n_1',m_1',n_2',m_2'}(s,t)dsdt \\ &= \int_0^{h_1}\int_0^{h_2} \mathscr{W}_{\alpha_1}(s)\mathscr{W}_{\alpha_2}(t)\psi^{h_1,\alpha_1}_{n_1,m_1}(s)\psi^{h_2,\alpha_2}_{n_2,m_2}(t)\psi^{h_1,\alpha_1}_{n_1',m_1'}(s)\psi^{h_2,\alpha_2}_{n_2',m_2'}(t)dsdt \\ &= \int_0^{h_1} \mathscr{W}_{\alpha_1}(s)\psi^{h_1,\alpha_1}_{n_1,m_1}(s)\psi^{h_1,\alpha_1}_{n_1',m_1'}(s)ds \int_0^{h_2} \mathscr{W}_{\alpha_2}(t)\psi^{h_2,\alpha_2}_{n_2,m_2}(t)\psi^{h_2,\alpha_2}_{n_2',m_2'}(t)dt \\ &= \delta_{n_1n_1'}\delta_{m_1m_1'}\delta_{n_2n_2'}\delta_{m_2m_2'}. \end{aligned}$$

□

We can express a function $\mathscr{U}(s,t) \in L^2([0,h_1)\times[0,h_2))$ in terms of FOGCW as

$$\mathscr{U}(s,t) = \sum_{n_1=1}^{2^{k_1-1}} \sum_{n_2=1}^{2^{k_2-1}} \sum_{m_1=0}^{\infty} \sum_{m_2=0}^{\infty} r_{n_1,n_2,m_1,m_2} \psi_{n_1,m_1}^{h_1,\alpha_1}(s) \psi_{n_2,m_2}^{h_2,\alpha_2}(t), \tag{12}$$

where $r_{n_1,n_2,m_1,m_2} \in \mathbb{R}$. Taking M_1-1 order in s and M_2-1 order in t, we have

$$\mathscr{U}(s,t) \approx \sum_{n_1=1}^{2^{k_1-1}} \sum_{n_2=1}^{2^{k_2-1}} \sum_{m_1=0}^{M_1-1} \sum_{m_2=0}^{M_2-1} r_{n_1,n_2,m_1,m_2} \psi_{n_1,m_1}^{h_1,\alpha_1}(s) \psi_{n_2,m_2}^{h_2,\alpha_2}(t),$$

$$\mathscr{U}(s,t) \approx \mathscr{U}_{k_1,k_2,M_1,M_2}^{\alpha_1,\alpha_2} = \Psi_{k_1,M_1}^{h_1,\alpha_1}(s)^T \cdot R \cdot \Psi_{k_2,M_2}^{h_2,\alpha_2}(t), \tag{13}$$

where

$$\Psi_{k,M}^{h_1,\alpha_1} = \left[\psi_{1,0}^{h_1,\alpha_1},\ldots,\psi_{1,M-1}^{h_1,\alpha_1},\psi_{2,0}^{h_1,\alpha_1},\ldots,\psi_{2,M-1}^{h_1,\alpha_1},\ldots,\psi_{2^{k-1},M-1}^{h_1,\alpha_1}\right]^T, \tag{14}$$

and R is a matrix of $2^{k_1-1}M_1 \times 2^{k_2-1}M_2$ order composed of FOGCW coefficients

$$\begin{aligned} r_{n_1,n_2,m_1,m_2} &= \left\langle \mathscr{U}(s,t), \psi_{n_1,m_1}^{h_1,\alpha_1}(s)\psi_{n_2,m_2}^{h_2,\alpha_2}(t)\right\rangle \\ &= \int_0^{h_1}\int_0^{h_2} \mathscr{W}_{\alpha_1,\alpha_2}(s,t)\mathscr{U}(s,t)\psi_{n_1,m_1}^{h_1,\alpha_1}(s)\psi_{n_2,m_2}^{h_2,\alpha_2}(t)dsdt, \end{aligned} \tag{15}$$

$$1 \le n_1 \le 2^{k_1-1}, 0 \le m_1 \le M_1-1, 1 \le n_2 \le 2^{k_2-1}, 0 \le m_2 \le M_2-1.$$

We have considered the following collocation points:

$$\begin{aligned} s_i &= h_1\left(\frac{2i-1}{2^{k_1}M_1}\right)^{\frac{1}{\alpha_1}},\ i = 1,2,\ldots,2^{k_1-1}M_1, \\ t_j &= h_2\left(\frac{2j-1}{2^{k_2}M_2}\right)^{\frac{1}{\alpha_2}},\ j = 1,2,\ldots,2^{k_2-1}M_2. \end{aligned} \tag{16}$$

Next theorem deals with the derivation of an exact formula for the RLFIO of FOGCW. It removes approximation error at the integral stage and improves the overall accuracy of the proposed method.

Theorem 1. $I^{\beta}\psi_{n,m}^{h,\alpha}(s) = \begin{cases} 0, & s \le a_1, \\ \mathscr{A}(s), & a_1 \le s < a_2, \\ \mathscr{A}(s)-\mathscr{B}(s), & s \ge a_2, \end{cases}$

where

$$\mathscr{A}(s) = \sum_{j=0}^{M-m-1} \sqrt{2m+1}\,2^{\frac{k-1}{2}}(-1)^j \binom{M-1-m}{j}\binom{M+m+j}{M-1-m} \sum_{q=0}^{m+j}\binom{m+j}{q}(-1)^{m+j-q}$$
$$\frac{2^{q(k-1)}}{h^{\alpha q}}(n-1)^{m+j-q}\frac{\Gamma(q\alpha+1)}{\Gamma(\beta+q\alpha+1)}s^{\beta+q\alpha}\left[1-\mathscr{I}\left(\frac{a_1}{s};q\alpha+1,\beta\right)\right],$$

$$\mathscr{B}(s)=\sum_{j=0}^{M-m-1}\sqrt{2m+1}2^{\frac{k-1}{2}}(-1)^j\binom{M-1-m}{j}\binom{M+m+j}{M-1-m}\sum_{q=0}^{m+j}\binom{m+j}{q}(-1)^{m+j-q}$$
$$\frac{2^{q(k-1)}}{h^{\alpha q}}(n-1)^{m+j-q}\frac{\Gamma(q\alpha+1)}{\Gamma(\beta+q\alpha+1)}s^{\beta+q\alpha}\left[1-\mathscr{I}\left(\frac{a_2}{s};q\alpha+1,\beta\right)\right],$$

with $a_1=h_1(\frac{n-1}{2^{k-1}})^{\frac{1}{\alpha}}$, $a_2=h_2(\frac{n}{2^{k-1}})^{\frac{1}{\alpha}}$.

Proof. We can rewrite FOGCW in (9) as

$$\begin{aligned}\psi_{n,m}^{h,\alpha}(s)=&2^{\frac{k-1}{2}}\sqrt{2m+1}\mathscr{P}_{m,M}\left(\frac{2^{k-1}s^{\alpha}}{h^{\alpha}}-n+1\right)(\mu_{a_1}(s)-\mu_{a_2}(s))\\ =&2^{\frac{k-1}{2}}\sqrt{2m+1}\sum_{j=0}^{M-m-1}(-1)^j\binom{M-1-m}{j}\binom{M+m+j}{M-m-1}\left(\frac{2^{k-1}s^{\alpha}}{h^{\alpha}}-n+1\right)^{m+j}\\ &(\mu_{a_1}(s)-\mu_{a_2}(s)).\end{aligned}$$

Applying Binomial theorem, we have

$$\begin{aligned}\psi_{n,m}^{h,\alpha}(s)=&2^{\frac{k-1}{2}}\sqrt{2m+1}\sum_{j=0}^{M-m-1}(-1)^j\binom{M-1-m}{j}\binom{M+m+j}{M-m-1}\sum_{q=0}^{m+j}\binom{m+j}{q}\\ &2^{q(k-1)}\frac{s^{\alpha q}}{h^{\alpha q}}(-1)^{m+j-q}(n-1)^{m+j-q}(\mu_{a_1}(s)-\mu_{a_2}(s)).\end{aligned}\tag{17}$$

Taking RLFIO on both sides of Equation (17) gives

$$\begin{aligned}I^{\beta}\psi_{n,m}^{h,\alpha}(s)=&2^{\frac{k-1}{2}}\sqrt{2m+1}\sum_{j=0}^{M-m-1}(-1)^j\binom{M-1-m}{j}\binom{M+m+j}{M-m-1}\sum_{q=0}^{m+j}\binom{m+j}{q}\\ &\frac{2^{q(k-1)}}{h^{\alpha q}}(-1)^{m+j-q}(n-1)^{m+j-q}(I^{\beta}(s^{\alpha q}\mu_{a_1}(s))-I^{\beta}(s^{\alpha q}\mu_{a_2}(s))).\end{aligned}$$

Using Lemma 1, we have

$$\begin{aligned}I^{\beta}\psi_{n,m}^{h,\alpha}(s)=&2^{\frac{k-1}{2}}\sqrt{2m+1}\sum_{j=0}^{M-m-1}(-1)^j\binom{M-1-m}{j}\binom{M+m+j}{M-m-1}\sum_{q=0}^{m+j}\binom{m+j}{q}\\ &\frac{2^{q(k-1)}}{h^{\alpha q}}(-1)^{m+j-q}(n-1)^{m+j-q}\left[\frac{\Gamma(q\alpha+1)}{\Gamma(\beta+q\alpha+1)}s^{\beta+q\alpha}\left(1-\mathscr{I}\left(\frac{a_1}{s};q\alpha+1,\beta\right)\right)\mu_{a_1}(s)\right.\\ &\left.-\frac{\Gamma(q\alpha+1)}{\Gamma(\beta+q\alpha+1)}s^{\beta+q\alpha}\left(1-\mathscr{I}\left(\frac{a_2}{s};q\alpha+1,\beta\right)\right)\mu_{a_2}(s)\right].\end{aligned}$$

Let us assume

$$\mathscr{A}(s)=\sum_{j=0}^{M-m-1}\sqrt{2m+1}2^{\frac{k-1}{2}}(-1)^j\binom{M-1-m}{j}\binom{M+m+j}{M-1-m}\sum_{q=0}^{m+j}\binom{m+j}{q}(-1)^{m+j-q}$$

$$\frac{2^{q(k-1)}}{h^{\alpha q}}(n-1)^{m+j-q}\frac{\Gamma(q\alpha+1)}{\Gamma(\beta+q\alpha+1)}s^{\beta+q\alpha}\left[1-\mathscr{I}\left(\frac{a_1}{s};q\alpha+1,\beta\right)\right],$$

$$\mathscr{B}(s)=\sum_{j=0}^{M-m-1}\sqrt{2m+1}2^{\frac{k-1}{2}}(-1)^j\binom{M-1-m}{j}\binom{M+m+j}{M-1-m}\sum_{q=0}^{m+j}\binom{m+j}{q}(-1)^{m+j-q}$$

$$\frac{2^{q(k-1)}}{h^{\alpha q}}(n-1)^{m+j-q}\frac{\Gamma(q\alpha+1)}{\Gamma(\beta+q\alpha+1)}s^{\beta+q\alpha}\left[1-\mathscr{I}\left(\frac{a_2}{s};q\alpha+1,\beta\right)\right],$$

we get

$$I^{\beta}\psi_{n,m}^{h,\alpha}(s)=\begin{cases}0, & s\le a_1,\\ \mathscr{A}(s), & a_1\le s<a_2,\\ \mathscr{A}(s)-\mathscr{B}(s), & s\ge a_2,\end{cases}$$

□

5 Error analysis

Here, we present the error analysis of the proposed method. Following the approach of [37], we have proved an error bound. First, let us define some notations:

$$\mathscr{X}_{k_1,k_2,M_1,M_2}^{\alpha_1,\alpha_2}=span\left(\psi_{n_1,m_1}^{h_1,\alpha_1}(s)\psi_{n_2,m_2}^{h_2,\alpha_2}(t)|1\le n_i\le 2^{k_i-1};0\le m_1\le M_i-1,i=1,2\right),$$

$$\mathscr{I}_{n_1}^{k_1}=\left[h_1\left(\frac{n_1-1}{2^{k_1-1}}\right)^{1/\alpha_1},h_1\left(\frac{n_1}{2^{k_1-1}}\right)^{1/\alpha_1}\right),$$

$$\mathscr{I}_{n_2}^{k_2}=\left[h_2\left(\frac{n_2-1}{2^{k_2-1}}\right)^{1/\alpha_2},h_2\left(\frac{n_2}{2^{k_2-1}}\right)^{1/\alpha_2}\right),$$

$\Omega=([0,h_1)\times[0,h_2))$, $\Lambda_{n_1,n_2}=\mathscr{I}_{n_1}^{k_1}\times\mathscr{I}_{n_2}^{k_2}$, $\Omega=\bigcup_{n_1=1}^{2^{k_1-1}}\bigcup_{n_2=1}^{2^{k_2-1}}\Lambda_{n_1,n_2}$, $\Lambda_{n_1,n_2}\cap\Lambda_{n_1',n_2'}=\emptyset$ for $(n_1,n_2)\neq(n_1',n_2')$, $|\frac{\partial^{i\alpha_1+j\alpha_2}}{\partial s^{i\alpha_1}\partial t^{j\alpha_2}}|\le f_{M_1,M_2}^{\alpha_1,\alpha_2}$ on Λ_{n_1,n_2}, $|\frac{\partial^{i\alpha_1+j\alpha_2}}{\partial s^{i\alpha_1}\partial t^{j\alpha_2}}|\le \mathscr{J}_{M_1,M_2}^{\alpha_1,\alpha_2}$ on Ω for $i=0,1,\ldots,M_1, j=0,1,\ldots,M_2$, and ${}^{C}D_t^{\beta}\mathscr{U}(s,t)=\frac{\partial^{\beta}\mathscr{U}(s,t)}{\partial t^{\beta}}$.
The next lemma quantifies the approximation error between the exact solution and its wavelet projection in the L^2-norm.

Lemma 4. *Let $\mathscr{V}(s,t)$ be the best approximation out of linear space $\mathscr{X}_{k_1,k_2,M_1,M_2}^{\alpha_1,\alpha_2}$. Also let $\frac{\partial^{i\alpha_1+j\alpha_2}u(s,t)}{\partial s^{i\alpha_1}\partial t^{j\alpha_2}}\in C(\Omega)$ for $i=0,1,\ldots,M_1, j=0,1,\ldots,M_2$, then the error bound by using FOGCW is given as*

$$\left|\left|\mathscr{U}(s,t)-\mathscr{V}(s,t)\right|\right|_{L^2(\Omega)}\le\frac{\mathscr{J}_{M_1,M_2}^{\alpha_1,\alpha_2}h_1^{M_1\alpha_1+\frac{1}{2}}h_2^{M_2\alpha_2+\frac{1}{2}}}{\Gamma(M_2\alpha_2+1)\Gamma(M_1\alpha_1+1)\sqrt{(2M_2\alpha_2+1)(2M_1\alpha_1+1)}}.$$

Proof. We define

$$\mathscr{Y}^{\alpha_1,\alpha_2}_{M_1,M_2}(s,t)=\sum_{p=1}^{M_1-1}\sum_{l=1}^{M_2-1}\frac{s^{p\alpha_1}t^{l\alpha_2}}{\Gamma(p\alpha_1+1)\Gamma(l\alpha_2+1)}\frac{\partial^{p\alpha_1+l\alpha_2}}{\partial s^{p\alpha_1}\partial t^{l\alpha_2}}\bigg|_{(0,0)}. \tag{18}$$

From generalized Taylor's formula, we have

$$\left|\mathscr{U}(s,t)-\mathscr{Y}^{\alpha_1,\alpha_2}_{M_1,M_2}(s,t)\right|\leq\frac{s^{M_1\alpha_1}t^{M_2\alpha_2}}{\Gamma(M_1\alpha_1+1)\Gamma(M_2\alpha_2+1)}f^{\alpha_1,\alpha_2}_{M_1,M_2}. \tag{19}$$

Since the domain Ω is the union of non-overlapping subdomains Λ_{n_1,n_2}, and using the properties of L^2-norm, we have

$$\begin{aligned}
\left\|\mathscr{U}(s,t)-\mathscr{V}(s,t)\right\|^2_{L^2(\Omega)}&=\sum_{n_1=1}^{2^{k_1-1}}\sum_{n_2=1}^{2^{k_2-1}}\left\|\mathscr{U}(s,t)-\mathscr{V}(s,t)\right\|^2_{L^2(\Lambda_{n_1,n_2})}\\
&\leq\sum_{n_1=1}^{2^{k_1-1}}\sum_{n_2=1}^{2^{k_2-1}}\left\|\mathscr{U}(s,t)-\mathscr{Y}^{\alpha_1,\alpha_2}_{M_1,M_2}(s,t)\right\|^2_{L^2(\Lambda_{n_1,n_2})}\\
&\leq\sum_{n_1=1}^{2^{k_1-1}}\sum_{n_2=1}^{2^{k_2-1}}\int_{\mathscr{I}^{k_1}_{n_1}}\int_{\mathscr{I}^{k_2}_{n_2}}\left(\frac{s^{M_1\alpha_1}t^{M_2\alpha_2}}{\Gamma(M_1\alpha_1+1)\Gamma(M_2\alpha_2+1)}f^{\alpha_1,\alpha_2}_{M_1,M_2}\right)^2dsdt\\
&\leq\int_0^{h_1}\int_0^{h_2}\left(\frac{s^{M_1\alpha_1}t^{M_2\alpha_2}}{\Gamma(M_1\alpha_1+1)\Gamma(M_2\alpha_2+1)}\mathscr{J}^{\alpha_1,\alpha_2}_{M_1,M_2}\right)^2dsdt\\
&\leq\left[\frac{\mathscr{J}^{\alpha_1,\alpha_2}_{M_1,M_2}h_1^{M_1\alpha_1+\frac{1}{2}}h_2^{M_2\alpha_2+\frac{1}{2}}}{\Gamma(M_2\alpha_2+1)\Gamma(M_1\alpha_1+1)\sqrt{(2M_2\alpha_2+1)(2M_1\alpha_1+1)}}\right]^2.
\end{aligned}$$

Thus

$$\left\|\mathscr{U}(s,t)-\mathscr{V}(s,t)\right\|_{L^2(\Omega)}\leq\frac{\mathscr{J}^{\alpha_1,\alpha_2}_{M_1,M_2}h_1^{M_1\alpha_1+\frac{1}{2}}h_2^{M_2\alpha_2+\frac{1}{2}}}{\Gamma(M_2\alpha_2+1)\Gamma(M_1\alpha_1+1)\sqrt{(2M_2\alpha_2+1)(2M_1\alpha_1+1)}}.$$

□

Lemma 5. *We have*

$$\left\|\frac{\partial^\beta\mathscr{U}(s,t)}{\partial t^\beta}-\frac{\partial^\beta\mathscr{V}(s,t)}{\partial t^\beta}\right\|_{L^2(\Omega)}\leq\frac{\mathscr{J}^{\alpha_1,\alpha_2}_{M_1,M_2}h_1^{M_1\alpha_1+\frac{1}{2}}h_2^{M_2\alpha_2-\beta+\frac{1}{2}}}{\Gamma(M_1\alpha_1+1)\Gamma(M_2\alpha_2+1-\beta)\sqrt{(2M_1\alpha_1+1)(2M_2\alpha_2+1-2\beta)}}.$$

Proof. Applying Caputo derivative with respect to t on both sides of Equation (19) and using it's properties, we have

$$\left|\frac{\partial^\beta\mathscr{U}(s,t)}{\partial t^\beta}-\frac{\partial^\beta}{\partial t^\beta}\mathscr{Y}^{\alpha_1,\alpha_2}_{M_1,M_2}(s,t)\right|\leq\frac{s^{M_1\alpha_1}t^{M_2\alpha_2-\beta}\Gamma(M_2\alpha_2+1)}{\Gamma(M_1\alpha_1+1)\Gamma(M_2\alpha_2+1)\Gamma(M_2\alpha_2+1-\beta)}f^{\alpha_1,\alpha_2}_{M_1,M_2}. \tag{20}$$

Since the domain Ω is the union of non-overlapping subdomains Λ_{n_1,n_2}, and using the properties of L^2-norm, we have

$$\left\|\frac{\partial^\beta\mathscr{U}(s,t)}{\partial t^\beta}-\frac{\partial^\beta\mathscr{V}(s,t)}{\partial t^\beta}\right\|^2_{L^2(\Omega)}=\sum_{n_1=1}^{2^{k_1-1}}\sum_{n_2=1}^{2^{k_2-1}}\left\|\frac{\partial^\beta\mathscr{U}(s,t)}{\partial t^\beta}-\frac{\partial^\beta\mathscr{V}(s,t)}{\partial t^\beta}\right\|^2_{L^2(\Lambda_{n_1,n_2})}$$

$$\leq \sum_{n_1=1}^{2^{k_1-1}} \sum_{n_2=1}^{2^{k_2-1}} \left\| \frac{\partial^\beta u(s,t)}{\partial t^\beta} - \frac{\partial^\beta \mathscr{Y}_{M_1,M_2}^{\alpha_1,\alpha_2}(s,t)}{\partial t^\beta} \right\|^2_{L^2(\Lambda_{n_1,n_2})}.$$

From Equation (20), we have

$$\begin{aligned}
\left\| \frac{\partial^\beta \mathscr{U}(s,t)}{\partial t^\beta} - \frac{\partial^\beta \mathscr{V}(s,t)}{\partial t^\beta} \right\|^2 &\leq \sum_{n_1=1}^{2^{k_1-1}} \sum_{n_2=1}^{2^{k_2-1}} \int_{\mathscr{I}_{n_1}^{k_1}} \int_{\mathscr{I}_{n_2}^{k_2}} \left(\frac{s^{M_1\alpha_1} t^{M_2\alpha_2-\beta} f_{M_1,M_2}^{\alpha_1,\alpha_2}}{\Gamma(M_1\alpha_1+1)\Gamma(M_2\alpha_2+1-\beta)} \right)^2 ds dt \\
&\leq \int_0^{h_1} \int_0^{h_2} \left(\frac{s^{M_1\alpha_1} t^{M_2\alpha_2-\beta} \mathscr{J}_{M_1,M_2}^{\alpha_1,\alpha_2}}{\Gamma(M_1\alpha_1+1)\Gamma(M_2\alpha_2+1-\beta)} \right)^2 ds dt \\
&\leq \left[\frac{\mathscr{J}_{M_1,M_2}^{\alpha_1,\alpha_2} h_1^{M_1\alpha_1+\frac{1}{2}} h_2^{M_2\alpha_2-\beta+\frac{1}{2}}}{\Gamma(M_1\alpha_1+1)\Gamma(M_2\alpha_2+1-\beta)\sqrt{(2M_1\alpha_1+1)(2M_2\alpha_2+1-2\beta)}} \right]^2.
\end{aligned}$$

$$\left\| \frac{\partial^\beta \mathscr{U}(s,t)}{\partial t^\beta} - \frac{\partial^\beta \mathscr{V}(s,t)}{\partial t^\beta} \right\|_{L^2(\Omega)} \leq \frac{\mathscr{J}_{M_1,M_2}^{\alpha_1,\alpha_2} h_1^{M_1\alpha_1+\frac{1}{2}} h_2^{M_2\alpha_2-\beta+\frac{1}{2}}}{\Gamma(M_1\alpha_1+1)\Gamma(M_2\alpha_2+1-\beta)\sqrt{(2M_1\alpha_1+1)(2M_2\alpha_2+1-2\beta)}}.$$

□

Lemma 6. *We have*

$$\left\| \frac{\partial \mathscr{U}(s,t)}{\partial s} - \frac{\partial \mathscr{V}(s,t)}{\partial s} \right\|_{L^2(\Omega)} \leq \frac{\mathscr{J}_{M_1,M_2}^{\alpha_1,\alpha_2} h_1^{M_1\alpha_1-\frac{1}{2}} h_2^{M_2\alpha_2+\frac{1}{2}}}{\Gamma(M_2\alpha_2+1)\Gamma(M_1\alpha_1)\sqrt{(2M_2\alpha_2+1)(2M_1\alpha_1-1)}},$$

$$\left\| \frac{\partial^2 \mathscr{U}(s,t)}{\partial s^2} - \frac{\partial^2 \mathscr{V}(s,t)}{\partial s^2} \right\|_{L^2(\Omega)} \leq \frac{\mathscr{J}_{M_1,M_2}^{\alpha_1,\alpha_2} h_1^{M_1\alpha_1-\frac{3}{2}} h_2^{M_2\alpha_2+\frac{1}{2}}}{\Gamma(M_2\alpha_2+1)\Gamma(M_1\alpha_1-1)\sqrt{(2M_2\alpha_2+1)(2M_1\alpha_1-3)}}.$$

Proof. The proof follows from Lemma 5. □

To justify the accuracy of the proposed FOGCW, we present the next theorem. It provides an explicit upper bound for the L^2-norm of the error under the assumption of Lemmas 4–6 and demonstrates how the truncation parameters M_1 and M_2 influence the accuracy of the proposed numerical approach.

Theorem 2. *The error bound* $(\mathscr{E}_{m_1,M_1}^{m_2,M_2})$ *is given as*

$$\begin{aligned}
\|\mathscr{E}_{m_1,M_1}^{m_2,M_2}\|_{L^2(\Omega)} \leq \mathscr{J}_{M_1,M_2}^{\alpha_1,\alpha_2} \Bigg(& \frac{h_1^{M_1\alpha_1+\frac{1}{2}} h_2^{M_2\alpha_2-\beta+\frac{1}{2}}}{\Gamma(M_1\alpha_1+1)\Gamma(M_2\alpha_2+1-\beta)\sqrt{(2M_1\alpha_1+1)(2M_2\alpha_2+1-2\beta)}} \\
& + \frac{\mathscr{L}_1 h_1^{M_1\alpha_1-\frac{3}{2}} h_2^{M_2\alpha_2+\frac{1}{2}}}{\Gamma(M_2\alpha_2+1)\Gamma(M_1\alpha_1-1)\sqrt{(2M_2\alpha_2+1)(2M_1\alpha_1-3)}}, \\
& + \frac{\mathscr{L}_2 h_1^{M_1\alpha_1-\frac{1}{2}} h_2^{M_2\alpha_2+\frac{1}{2}}}{\Gamma(M_2\alpha_2+1)\Gamma(M_1\alpha_1)\sqrt{(2M_2\alpha_2+1)(2M_1\alpha_1-1)}} \\
& + \frac{\mathscr{L}_3 h_1^{M_1\alpha_1+\frac{1}{2}} h_2^{M_2\alpha_2+\frac{1}{2}}}{\Gamma(M_2\alpha_2+1)\Gamma(M_1\alpha_1+1)\sqrt{(2M_2\alpha_2+1)(2M_1\alpha_1+1)}} \Bigg),
\end{aligned}$$

where $\|\mathscr{P}\| \leq \mathscr{L}_1$, $\|\mathscr{Q}\| \leq \mathscr{L}_2$, *and* $\|\mathscr{R}\| \leq \mathscr{L}_3$.

Proof. We have

$$\|\mathscr{E}^{m_2,M_2}_{m_1,M_1}\|_{L^2(\Omega)} = \left\| \frac{\partial^\beta \mathscr{V}(s,t)}{\partial t^\beta} - \mathscr{P}\frac{\partial^2 \mathscr{V}(s,t)}{\partial s^2} - \mathscr{Q}\frac{\partial \mathscr{V}(s,t)}{\partial s} + \mathscr{R}\mathscr{U}(s,t) - \mathscr{F}(s,t) \right\|.$$

Using Equation (5), we get

$$\begin{aligned}
\|\mathscr{E}^{m_2,M_2}_{m_1,M_1}\|_{L^2(\Omega)} =& \left\| \frac{\partial^\beta \mathscr{V}(s,t)}{\partial t^\beta} - \mathscr{P}\frac{\partial^2 \mathscr{V}(s,t)}{\partial s^2} - \mathscr{Q}\frac{\partial \mathscr{V}(s,t)}{\partial s} + \mathscr{R}\mathscr{V}(s,t) \right. \\
& \left. - \frac{\partial^\beta \mathscr{U}(s,t)}{\partial t^\beta} + \mathscr{P}\frac{\partial^2 \mathscr{U}(s,t)}{\partial s^2} + \mathscr{Q}\frac{\partial \mathscr{U}(s,t)}{\partial s} - \mathscr{R}\mathscr{U}(s,t) \right\| \\
\leq & \left\| \frac{\partial^\beta \mathscr{V}(s,t)}{\partial t^\beta} - \frac{\partial^\beta \mathscr{U}(s,t)}{\partial t^\beta} \right\| + \|\mathscr{P}\| \left\| \frac{\partial^2 \mathscr{V}(s,t)}{\partial s^2} - \frac{\partial^2 \mathscr{U}(s,t)}{\partial s^2} \right\| \\
& + \|\mathscr{Q}\| \left\| \frac{\partial \mathscr{V}(s,t)}{\partial s} - \frac{\partial \mathscr{U}(s,t)}{\partial s} \right\| + \|\mathscr{R}\| \|\mathscr{V}(s,t) - \mathscr{U}(s,t)\|
\end{aligned}$$

From Lemmas 4, 5 and 6, we have

$$\begin{aligned}
\|\mathscr{E}^{m_2,M_2}_{m_1,M_1}\|_{L^2(\Omega)} \leq & \frac{\mathscr{J}^{\alpha_1,\alpha_2}_{M_1,M_2} h_1^{M_1\alpha_1+\frac{1}{2}} h_2^{M_2\alpha_2-\beta+\frac{1}{2}}}{\Gamma(M_1\alpha_1+1)\Gamma(M_2\alpha_2+1-\beta)\sqrt{(2M_1\alpha_1+1)(2M_2\alpha_2+1-2\beta)}} \\
& + \frac{\mathscr{L}_1 \mathscr{J}^{\alpha_1,\alpha_2}_{M_1,M_2} h_1^{M_1\alpha_1-\frac{3}{2}} h_2^{M_2\alpha_2+\frac{1}{2}}}{\Gamma(M_2\alpha_2+1)\Gamma(M_1\alpha_1-1)\sqrt{(2M_2\alpha_2+1)(2M_1\alpha_1-3)}}, \\
& + \frac{\mathscr{L}_2 \mathscr{J}^{\alpha_1,\alpha_2}_{M_1,M_2} h_1^{M_1\alpha_1-\frac{1}{2}} h_2^{M_2\alpha_2+\frac{1}{2}}}{\Gamma(M_2\alpha_2+1)\Gamma(M_1\alpha_1)\sqrt{(2M_2\alpha_2+1)(2M_1\alpha_1-1)}} \\
& + \frac{\mathscr{L}_3 \mathscr{J}^{\alpha_1,\alpha_2}_{M_1,M_2} h_1^{M_1\alpha_1+\frac{1}{2}} h_2^{M_2\alpha_2+\frac{1}{2}}}{\Gamma(M_2\alpha_2+1)\Gamma(M_1\alpha_1+1)\sqrt{(2M_2\alpha_2+1)(2M_1\alpha_1+1)}}.
\end{aligned}$$

Thus

$$\begin{aligned}
\|\mathscr{E}^{m_2,M_2}_{m_1,M_1}\|_{L^2(\Omega)} \leq & \mathscr{J}^{\alpha_1,\alpha_2}_{M_1,M_2} \left(\frac{h_1^{M_1\alpha_1+\frac{1}{2}} h_2^{M_2\alpha_2-\beta+\frac{1}{2}}}{\Gamma(M_1\alpha_1+1)\Gamma(M_2\alpha_2+1-\beta)\sqrt{(2M_1\alpha_1+1)(2M_2\alpha_2+1-2\beta)}} \right. \\
& + \frac{\mathscr{L}_1 h_1^{M_1\alpha_1-\frac{3}{2}} h_2^{M_2\alpha_2+\frac{1}{2}}}{\Gamma(M_2\alpha_2+1)\Gamma(M_1\alpha_1-1)\sqrt{(2M_2\alpha_2+1)(2M_1\alpha_1-3)}}, \\
& + \frac{\mathscr{L}_2 h_1^{M_1\alpha_1-\frac{1}{2}} h_2^{M_2\alpha_2+\frac{1}{2}}}{\Gamma(M_2\alpha_2+1)\Gamma(M_1\alpha_1)\sqrt{(2M_2\alpha_2+1)(2M_1\alpha_1-1)}} \\
& \left. + \frac{\mathscr{L}_3 h_1^{M_1\alpha_1+\frac{1}{2}} h_2^{M_2\alpha_2+\frac{1}{2}}}{\Gamma(M_2\alpha_2+1)\Gamma(M_1\alpha_1+1)\sqrt{(2M_2\alpha_2+1)(2M_1\alpha_1+1)}} \right).
\end{aligned}$$

□

It follows that as $M_1, M_2 \to \infty$

$$\|\mathscr{E}^{m_2,M_2}_{m_1,M_1}\|_{L^2(\Omega)} \to 0.$$

Also if k_1, $k_2 \to \infty$ then

$$\left|h_1\left(\frac{n_1}{2^{k_1-1}}\right)^{\frac{1}{\alpha_1}} - h_1\left(\frac{n_1-1}{2^{k_1-1}}\right)^{\frac{1}{\alpha_1}}\right| \to 0, \left|h_2\left(\frac{n_2}{2^{k_2-1}}\right)^{\frac{1}{\alpha_2}} - h_2\left(\frac{n_2-1}{2^{k_2-1}}\right)^{\frac{1}{\alpha_2}}\right| \to 0.$$

This implies

$$\|\mathscr{E}^{m_2,M_2}_{m_1,M_1}\|_{L^2(\Omega)} \to 0.$$

6 Numerical examples

Here we have taken six numerical examples to test the correctness of the proposed method. The following formula is used to measure the absolute error and maximum absolute error:

$$\text{Absolute error} = |\mathscr{V}(s,t) - \mathscr{U}(s,t)|, \qquad \mathscr{E}_\infty = \max|\mathscr{V}(s_i,t_j) - \mathscr{U}(s_i,t_j)|. \tag{21}$$

The convergence rate (CR) in space and time is obtained by using the formulas:

$$\text{CR} = \frac{\log(\text{error}(M_1)/\text{error}(2M_1))}{\log(2)}, \qquad \text{CR} = \frac{\log(\text{error}(M_2)/\text{error}(2M_2))}{\log(2)},$$

where errors are taken by the $\mathscr{E}_\infty$ norm with respect to M_1 and M_2.

Example 1. Consider the following homogeneous time fractional BSE [23]:

$$\frac{\partial^\beta \mathscr{U}(s,t)}{\partial t^\beta} = \frac{1}{2}\sigma^2\frac{\partial^2\mathscr{U}(s,t)}{\partial s^2} + (r - \frac{\sigma^2}{2})\frac{\partial\mathscr{U}(s,t)}{\partial s} - r\mathscr{U}(s,t) + \mathscr{F}(s,t), \tag{22}$$

with I.C and B.Cs

$$\begin{aligned}
&\mathscr{U} = s^2(1-s) \ \text{ on } \ \Omega_b = \{(s,0)|0 \le s \le 1\},\\
&\mathscr{U} = 0 \ \text{ on } \ \Omega_l = \{(0,t)|0 \le t \le 1\},\\
&\mathscr{U} = 0 \ \text{ on } \ \Omega_r = \{(1,t)|0 \le t \le 1\}.
\end{aligned}$$

The source function $\mathscr{F}(s,t)$ is chosen so that the exact solution of the given problem is $\mathscr{U}(s,t) = (t+1)^2 s^2(1-s)$. We have solved the above example by using FOGCW. Table 5 compared the absolute error of our method with the method in [23] for different values of β. It can be clearly observed from the table that our method gives better results. The absolute error for different values of (α_1, α_2) are reported in Table 6. From the table, it can be seen that (α_1, α_2)=(0.5,0.5) is the best case among all considered cases. Table 7 shows the maximum absolute errors, CR, and CPU time at $k_1 = 2$, $k_2 = 1$, and $\alpha_1 = \alpha_2 = 0.5$. Figure 1 shows the plots of numerical and absolute errors for (α_1, α_2)=(0.5,0.5) and $\beta = 0.5$.

Table 5: Absolute error of Example 1 with $k_1 = k_2 = 1, M_1 = 4, M_2 = 8, \alpha_1 = \alpha_2 = 1$

(s,t)	Proposed method(FOGCW)			Method in [23]		
	$\beta = 0.4$	$\beta = 0.6$	$\beta = 0.8$	$\beta = 0.4$	$\beta = 0.6$	$\beta = 0.8$
(0.1,0.1)	$1.95 \cdot 10^{-19}$	$3.90 \cdot 10^{-19}$	$2.16 \cdot 10^{-20}$	$1.63 \cdot 10^{-18}$	$7.36 \cdot 10^{-18}$	$8.23 \cdot 10^{-19}$
(0.3,0.3)	0	$2.77 \cdot 10^{-18}$	$2.08 \cdot 10^{-18}$	$2.28 \cdot 10^{-17}$	$1.80 \cdot 10^{-17}$	$3.37 \cdot 10^{-17}$
(0.5,0.5)	0	$8.32 \cdot 10^{-18}$	$2.77 \cdot 10^{-19}$	$7.89 \cdot 10^{-17}$	$3.60 \cdot 10^{-17}$	$6.18 \cdot 10^{-19}$
(0.7,0.7)	$5.55 \cdot 10^{-17}$	$1.66 \cdot 10^{-17}$	0	$7.58 \cdot 10^{-17}$	$1.51 \cdot 10^{-16}$	$3.47 \cdot 10^{-17}$
(0.9,0.9)	$5.55 \cdot 10^{-17}$	$1.66 \cdot 10^{-17}$	$1.38 \cdot 10^{-17}$	$1.79 \cdot 10^{-16}$	$5.81 \cdot 10^{-16}$	$1.15 \cdot 10^{-16}$

Table 6: Maximum absolute error of Example 1 with $k_1 = 2, k_2 = 1, M_1 = M_2 = 4, \beta = 0.5$

$\alpha_1 \backslash \alpha_2$	0.25	0.5	0.75	1	1.25	1.5
0.25	$8.81 \cdot 10^{-4}$	$6.60 \cdot 10^{-5}$	$7.59 \cdot 10^{-5}$	$6.60 \cdot 10^{-5}$	$7.42 \cdot 10^{-5}$	$1.67 \cdot 10^{-4}$
0.5	$8.43 \cdot 10^{-4}$	$2.88 \cdot 10^{-15}$	$3.12 \cdot 10^{-5}$	$3.16 \cdot 10^{-15}$	$4.93 \cdot 10^{-5}$	$1.67 \cdot 10^{-4}$
0.75	$8.49 \cdot 10^{-4}$	$7.73 \cdot 10^{-6}$	$3.07 \cdot 10^{-5}$	$7.73 \cdot 10^{-6}$	$4.68 \cdot 10^{-5}$	$1.67 \cdot 10^{-4}$
1.0	$8.49 \cdot 10^{-4}$	$6.29 \cdot 10^{-15}$	$3.13 \cdot 10^{-5}$	$6.41 \cdot 10^{-15}$	$4.93 \cdot 10^{-5}$	$1.67 \cdot 10^{-4}$
1.25	$8.46 \cdot 10^{-4}$	$1.91 \cdot 10^{-5}$	$3.95 \cdot 10^{-5}$	$1.91 \cdot 10^{-5}$	$6.85 \cdot 10^{-5}$	$1.68 \cdot 10^{-4}$
1.5	$8.40 \cdot 10^{-4}$	$4.49 \cdot 10^{-5}$	$6.18 \cdot 10^{-5}$	$4.60 \cdot 10^{-5}$	$9.21 \cdot 10^{-5}$	$1.91 \cdot 10^{-4}$

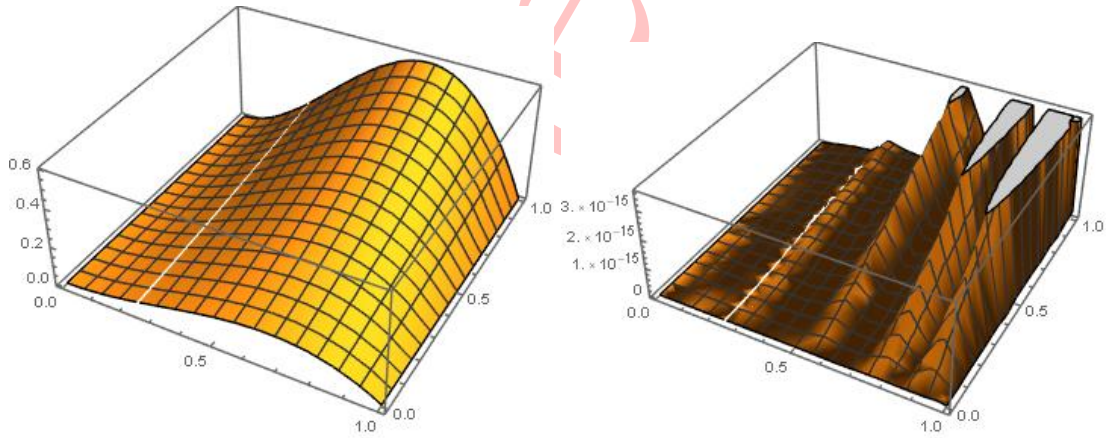

(a) **(b)**

Figure 1: (a) Plot of numerical solution using FOGCW with $k_1 = 2$, $k_2 = 1$, $M_1 = M_2 = 4$, $\alpha_1 = \alpha_2 = 0.5$, and $\beta = 0.5$, (b) plot of absolute errors using FOGCW with $k_1 = 2$, $k_2 = 1$, $M_1 = M_2 = 4$, $\alpha_1 = \alpha_2 = 0.5$, and $\beta = 0.5$ for Example 1

Example 2. Consider the following non homogeneous time fractional BSE [28]:

$$\frac{\partial^{\beta} \mathscr{U}(s,t)}{\partial t^{\beta}} = \frac{1}{2}\sigma^2 \frac{\partial^2 \mathscr{U}(s,t)}{\partial s^2} + (r - \frac{\sigma^2}{2}) \frac{\partial \mathscr{U}(s,t)}{\partial s} - r\mathscr{U}(s,t) + \mathscr{F}(s,t), \tag{23}$$

with I.C and B.Cs

$$\mathscr{U} = \sin(\pi s) + 1 \ \text{ on } \ \Omega_b = \{(s,0) | 0 \leq s \leq 1\},$$

Table 7: Maximum absolute errors, CR, and CPU time at $k_1 = 2$, $k_2 = 1$, and $\alpha_1 = \alpha_2 = 0.5$ for Example 1

	$M_2 = 2$	$M_2 = 4$	$M_2 = 8$	$M_2 = 16$
$\beta = 0.5, M_1 = 4$	$6.96 \cdot 10^{-14}$	$2.88 \cdot 10^{-15}$	$5.10 \cdot 10^{-16}$	$4.72 \cdot 10^{-18}$
CR	–	4.59	2.49	6.75
CPU(s)	5.12	26.40	28.18	36.10
$\beta = 0.7, M_1 = 4$	$2.52 \cdot 10^{-14}$	$3.16 \cdot 10^{-15}$	$8.33 \cdot 10^{-16}$	$4.16 \cdot 10^{-18}$
CR	–	2.99	1.92	7.64
CPU(s)	6.95	27.92	25.98	37.02

$$\mathscr{U} = t^3 + 1 \text{ on } \Omega_l = \{(0,t)|0 \le t \le 1\},$$
$$\mathscr{U} = t^3 + 1 \text{ on } \Omega_r = \{(1,t)|0 \le t \le 1\},$$

where

$$\mathscr{F}(s,t) = \left(\frac{6}{\Gamma(4-\beta)}t^{3-\beta} + rt^3 + r\right)(\sin(\pi s)+1) + \frac{1}{2}\pi^2\sigma^2(t^3+1)\sin(\pi s) - (r - \frac{1}{2}\sigma^2)\pi(t^3+1)\cos(\pi s).$$

The exact solution of this problem is $\mathscr{U}(s,t) = (t^3+1)(\sin(\pi s)+1)$. Following [23], we have taken $\beta = 0.5, 0.7$. We have applied the proposed method to solve Example 2. Table 8 shows the comparison of maximum absolute errors for different values of (α_1, α_2). The cases (α_1, α_2)=(1,0.5) and (1,1) give better solutions among all considered cases. Table 9 compared the maximum absolute errors of the proposed method with those of methods in [28] for (α_1, α_2)=(1,0.5) and $k_1 = k_2 = 1$. From this table, it is clear that the proposed method performs well. We have taken the step sizes $\delta x = \frac{1}{3000}$ and $\delta t = \frac{1}{20}, \frac{1}{40}, \frac{1}{80}$, and $\frac{1}{120}$ for SCFD and ECFD. Table 10 shows the maximum absolute errors, CR, and CPU time at $k_1 = k_2 = 1$ and $\alpha_1 = \alpha_2 = 1$. Figure 2 shows the plots of numerical and absolute errors of $\alpha_1 = 1, \alpha_2 = 0.5, \beta = 0.5$.

Table 8: Comparison of maximum absolute errors of Example 2 with $k_1 = k_2 = 1, M_1 = M_2 = 8, \beta = 0.5$

$\alpha_1 \backslash \alpha_2$		0.25	0.5	0.75	1	1.25	1.5
0.25	Method in [23]	$6.23 \cdot 10^{-3}$	$6.21 \cdot 10^{-3}$	$6.20 \cdot 10^{-3}$	$6.21 \cdot 10^{-3}$	$6.24 \cdot 10^{-3}$	$6.25 \cdot 10^{-3}$
	Proposed method	$1.23 \cdot 10^{-5}$	$3.16 \cdot 10^{-3}$	$1.78 \cdot 10^{-5}$	$3.16 \cdot 10^{-3}$	$3.16 \cdot 10^{-3}$	$3.16 \cdot 10^{-3}$
0.5	Method in [23]	$3.91 \cdot 10^{-4}$	$6.03 \cdot 10^{-5}$	$6.32 \cdot 10^{-5}$	$6.03 \cdot 10^{-5}$	$3.43 \cdot 10^{-5}$	$1.10 \cdot 10^{-4}$
	Proposed method	$1.54 \cdot 10^{-5}$	$2.72 \cdot 10^{-5}$	$2.68 \cdot 10^{-5}$	$2.72 \cdot 10^{-5}$	$2.67 \cdot 10^{-5}$	$5.64 \cdot 10^{-5}$
0.75	Method in [23]	$3.89 \cdot 10^{-4}$	$9.22 \cdot 10^{-7}$	$1.82 \cdot 10^{-5}$	$1.05 \cdot 10^{-6}$	$3.43 \cdot 10^{-5}$	$1.10 \cdot 10^{-4}$
	Proposed Method	$2.12 \cdot 10^{-5}$	$2.12 \cdot 10^{-7}$	$4.10 \cdot 10^{-7}$	$2.12 \cdot 10^{-7}$	$1.30 \cdot 10^{-5}$	$5.64 \cdot 10^{-5}$
1	Method in [23]	$3.90 \cdot 10^{-4}$	$1.71 \cdot 10^{-7}$	$1.50 \cdot 10^{-6}$	$1.81 \cdot 10^{-6}$	$3.43 \cdot 10^{-5}$	$1.10 \cdot 10^{-4}$
	Proposed method	$2.11 \cdot 10^{-5}$	$4.12 \cdot 10^{-8}$	$2.81 \cdot 10^{-7}$	$4.12 \cdot 10^{-8}$	$1.30 \cdot 10^{-5}$	$5.64 \cdot 10^{-5}$
1.25	Method in [23]	$2.69 \cdot 10^{-4}$	$2.80 \cdot 10^{-4}$	$2.84 \cdot 10^{-4}$	$2.80 \cdot 10^{-4}$	$2.59 \cdot 10^{-4}$	$1.10 \cdot 10^{-4}$
	Proposed method	$2.22 \cdot 10^{-5}$	$9.97 \cdot 10^{-7}$	$1.32 \cdot 10^{-6}$	$9.97 \cdot 10^{-7}$	$1.29 \cdot 10^{-5}$	$5.63 \cdot 10^{-5}$
1.5	Method in [23]	$1.69 \cdot 10^{-3}$	$1.80 \cdot 10^{-3}$	$1.81 \cdot 10^{-3}$	$1.80 \cdot 10^{-3}$	$1.77 \cdot 10^{-3}$	$1.75 \cdot 10^{-3}$
	Proposed method	$2.27 \cdot 10^{-5}$	$1.66 \cdot 10^{-6}$	$1.90 \cdot 10^{-6}$	$1.66 \cdot 10^{-6}$	$1.24 \cdot 10^{-5}$	$5.59 \cdot 10^{-5}$

Table 9: Comparison of maximum absolute errors with $k_1 = k_2 = 1$, (α_1, α_2)=(1,0.5)

(M_1, M_2)	Proposed method		SCFD scheme [28]		ECFD scheme [28]	
	$\beta = 0.5$	$\beta = 0.7$	$\beta = 0.5$	$\beta = 0.7$	$\beta = 0.5$	$\beta = 0.7$
(5, 8)	$5.26 \cdot 10^{-8}$	$5.24 \cdot 10^{-8}$	$1.81 \cdot 10^{-07}$	$1.82 \cdot 10^{-07}$	$8.24 \cdot 10^{-5}$	$2.32 \cdot 10^{-4}$
(5, 9)	$6.69 \cdot 10^{-12}$	$6.54 \cdot 10^{-12}$	$3.22 \cdot 10^{-09}$	$3.21 \cdot 10^{-09}$	$1.47 \cdot 10^{-5}$	$4.74 \cdot 10^{-5}$
(5,10)	$1.01 \cdot 10^{-12}$	$1.00 \cdot 10^{-12}$	$1.85 \cdot 10^{-09}$	$1.85 \cdot 10^{-09}$	$2.63 \cdot 10^{-6}$	$9.65 \cdot 10^{-6}$
(5,11)	$3.71 \cdot 10^{-13}$	$3.82 \cdot 10^{-13}$	$2.35 \cdot 10^{-11}$	2.33×10^{-11}	$4.68 \cdot 10^{-7}$	$1.96 \cdot 10^{-6}$

Table 10: Maximum absolute errors, CR, and CPU time at $k_1 = k_2 = 1$, and $\alpha_1 = \alpha_2 = 1$ for Example 2

	$M_2 = 2$	$M_2 = 4$	$M_2 = 8$	$M_2 = 16$
$\beta = 0.5, M_1 = 5$	$4.14 \cdot 10^{-1}$	$1.46 \cdot 10^{-2}$	$1.43 \cdot 10^{-5}$	$2.04 \cdot 10^{-8}$
CR	–	4.82	9.99	9.45
CPU(s)	6.92	29.40	29.18	38.10
$\beta = 0.7, M_1 = 5$	$2.01 \cdot 10^{-1}$	$3.31 \cdot 10^{-3}$	$1.39 \cdot 10^{-5}$	$2.13 \cdot 10^{-8}$
CR	–	5.92	7.89	9.35
CPU(s)	5.85	28.92	26.76	36.13

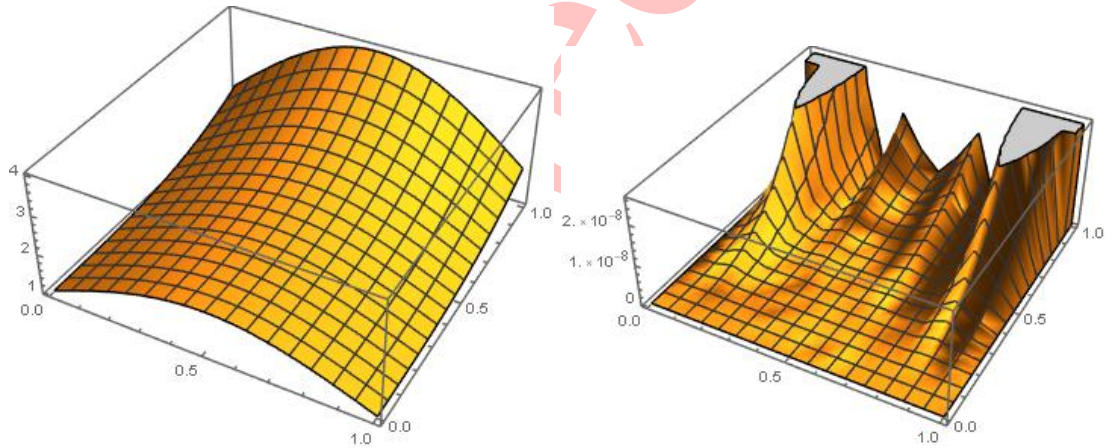

(a) **(b)**

Figure 2: (a) Plot of numerical solution using FOGCW with $k_1 = k_2 = 1$, $M_1 = M_2 = 8$, $\alpha_1 = 1$, $\alpha_2 = 1$, and $\beta = 0.5$, (b) plot of absolute errors using FOGCW with $k_1 = k_2 = 1$, $M_1 = M_2 = 8$, $\alpha_1 = 1$, $\alpha_2 = 1$, and $\beta = 0.5$ for Example 2

Example 3. Consider the following non homogeneous time fractional BSE [29]:

$$\frac{\partial^\beta \mathscr{U}(s,t)}{\partial t^\beta} = \frac{1}{2}\sigma^2 \frac{\partial^2 \mathscr{U}(s,t)}{\partial s^2} + (r - \frac{\sigma^2}{2}) \frac{\partial \mathscr{U}(s,t)}{\partial s} - r\mathscr{U}(s,t) + \mathscr{F}(s,t), \tag{24}$$

with I.C and B.Cs

$$\mathscr{U} = s^3 + s^2 + 1 \text{ on } \Omega_b = \{(s,0) | 0 \le s \le 1\},$$

$$\mathscr{U} = (1+t)^2 \text{ on } \Omega_l = \{(0,t)|0 \le t \le 1\},$$
$$\mathscr{U} = 3(1+t)^2 \text{ on } \Omega_r = \{(1,t)|0 \le t \le 1\},$$

where

$$\mathscr{F}(s,t) = \left(\frac{2t^{2-\beta}}{\Gamma(3-\beta)} + \frac{2t^{1-\beta}}{\Gamma(2-\beta)}\right)(s^3+s^2+1) - (t+1)^2$$
$$\left(\frac{\sigma^2}{2}(2+6s) + (r-\frac{\sigma^2}{2})(2s+3s^2) - r(s^3+s^2+1)\right).$$

Here $r = 0.5, \sigma = \sqrt{2}$. The exact solution of this problem is $(1+t)^2(s^3+s^2+1)$. We have compared the maximum absolute error obtained by the proposed method with that of methods in [30] for β = 0.1, 0.5, and 0.7. From Table 11, it can be observed that the proposed method uses a small number of basis functions and provides better results. From Table 12, we can see that the proposed method performs better than the methods presented in [24–27, 31]. Table 14 compared the proposed method with the method in [29] for different values of α with $M_1 = 5, M_2 = 3$. Table 13 shows the maximum absolute errors, CR, and CPU time at $k_1 = 1$, $k_2 = 1$, $\alpha_1 = 1$, and $\alpha_2 = \beta$. In Figure 3, we have shown the plots of numerical and absolute errors for $k_1 = k_2 = 1$, $M_1 = 4$, $M_2 = 3$, $\alpha_1 = 1$, $\alpha_1 = 1, \alpha_2 = 1$, and $\beta = 0.5$.

Table 11: Comparison of maximum absolute errors for different values of β

$\beta = 0.1$		$\beta = 0.5$		$\beta = 0.7$	
Method in [30]	Proposed method	Method in [30]	Proposed method	Method in [30]	Proposed method
$M_1 = 100, M_2 = 8192$	$M_1 = 5, M_2 = 3$	$M_1 = 100, M_2 = 4096$	$M_1 = 4, M_2 = 3$	$M_1 = 100, M_2 = 4096$	$M_1 = 4, M_2 = 3$
$3.15 \cdot 10^{-9}$	$3.55 \cdot 10^{-15}$	$2.97 \cdot 10^{-7}$	$3.55 \cdot 10^{-15}$	$1.62 \cdot 10^{-5}$	$1.77 \cdot 10^{-15}$

Table 12: Comparison of maximum absolute errors using different methods

$\beta = 0.7$		$\beta = 0.7$		$\beta = 0.7$	
Method in [25]	Method in [26]	Method in [24]	Method in [31]	Method in [27]	Proposed method
$\tau = \frac{1}{320}, \mathscr{N} = 100$	$\tau = \frac{1}{320}, \mathscr{N} = 100$	$\tau = \frac{1}{160}, \mathscr{N} = 100$	$\tau = \frac{1}{160}, \mathscr{N} = 100$	$\mathscr{N} = 5, \mathscr{M} = 320$	$M_1 = 4, M_2 = 3$
$9.64 \cdot 10^{-9}$	$8.24 \cdot 10^{-6}$	$1.00 \cdot 10^{-4}$	$9.96 \cdot 10^{-5}$	$6.15 \cdot 10^{-5}$	$1.77 \cdot 10^{-15}$

Table 13: Maximum absolute errors, CR, and CPU time at $k_1 = k_2 = 1$, $\alpha_1 = 1$, and $\alpha_2 = \beta$ for Example 3

	$M_2 = 2$	$M_2 = 4$	$M_2 = 8$	$M_2 = 16$
$\beta = 0.2, M_1 = 2$	$4.07 \cdot 10^{-2}$	$4.72 \cdot 10^{-3}$	$2.16 \cdot 10^{-7}$	$2.64 \cdot 10^{-12}$
CR	–	3.11	12.29	16.32
CPU(s)	5.92	30.40	29.18	37.10
$\beta = 0.6, M_1 = 2$	$6.74 \cdot 10^{-2}$	$1.03 \cdot 10^{-3}$	$4.24 \cdot 10^{-5}$	$3.03 \cdot 10^{-6}$
CR	–	6.01	4.61	3.80
CPU(s)	5.95	29.92	26.98	36.02

Table 14: Comparison of absolute error for Example 3 with $k_1 = k_2 = 1, M_1 = 5, M_2 = 3, \alpha_1 = \alpha_2 = 1$

(s,t)	Proposed method		Method in [29]	
	$\beta = 0.2$	$\beta = 0.6$	$\beta = 0.2$	$\beta = 0.6$
(0.1,0.1)	$2.22 \cdot 10^{-16}$	0	$5.10 \cdot 10^{-15}$	$6.66 \cdot 10^{-16}$
(0.2,0.2)	0	0	$5.99 \cdot 10^{-15}$	$1.11 \cdot 10^{-15}$
(0.3,0.3)	$4.44 \cdot 10^{-16}$	$4.44 \cdot 10^{-16}$	$9.32 \cdot 10^{-15}$	$2.66 \cdot 10^{-15}$
(0.4,0.4)	$4.44 \cdot 10^{-16}$	$8.88 \cdot 10^{-16}$	$2.66 \cdot 10^{-14}$	$2.22 \cdot 10^{15}$
(0.5,0.5)	$4.44 \cdot 10^{-16}$	$4.44 \cdot 10^{-16}$	$2.66 \cdot 10^{-15}$	$1.15 \cdot 10^{-14}$
(0.6,0.6)	$8.88 \cdot 10^{-16}$	0	$1.03 \cdot 10^{-13}$	$1.06 \cdot 10^{-14}$

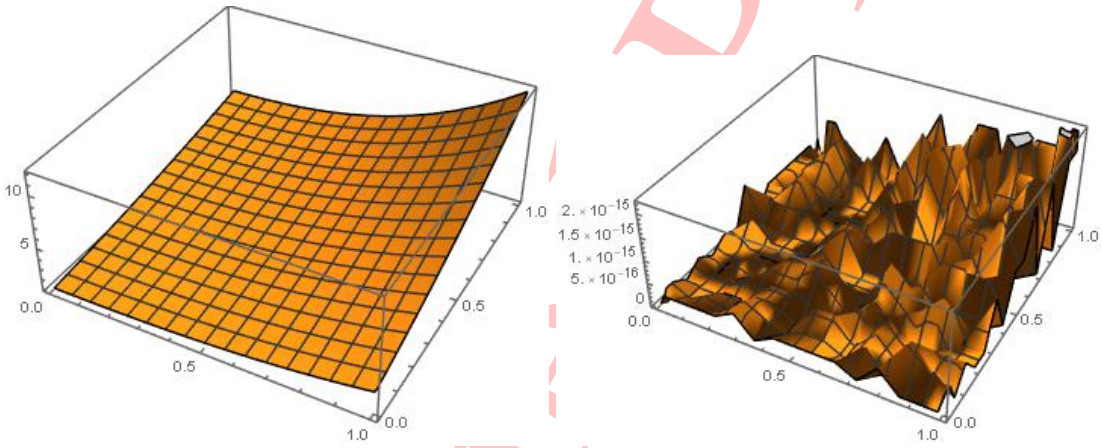

(a) **(b)**

Figure 3: (a) Plot of numerical solution using FOGCW with $k_1 = k_2 = 1$, $M_1 = 4$, $M_2 = 3$, $\alpha_1 = 1, \alpha_2 = 1$, and $\beta = 0.5$, (b) plot of absolute errors using FOGCW with $k_1 = k_2 = 1$, $M_1 = 4$, $M_2 = 3$, $\alpha_1 = 1, \alpha_2 = 1$, and $\beta = 0.5$ for Example 3

Example 4. Consider the following non homogeneous time fractional BSE [23]:

$$\frac{\partial^\beta \mathscr{U}(s,t)}{\partial t^\beta} = \frac{1}{2}\sigma^2 s^2 \frac{\partial^2 \mathscr{U}(s,t)}{\partial s^2} + rs\frac{\partial \mathscr{U}(s,t)}{\partial s} - r\mathscr{U}(s,t) + \mathscr{F}(s,t), \tag{25}$$

with I.C and B.Cs

$$\begin{aligned} \mathscr{U} &= e^s + s + 2 \ \text{ on } \ \Omega_b = \{(s,0) | 0 \le s \le 1\}, \\ \mathscr{U} &= t^\beta + 2 \ \text{ on } \ \Omega_l = \{(0,t) | 0 \le t \le 1\}, \\ \mathscr{U} &= t^\beta + e + 3 \ \text{ on } \ \Omega_r = \{(1,t) | 0 \le t \le 1\}. \end{aligned}$$

Here $r = 0.06$, $\sigma = 0.1$. The source function $\mathscr{F}(s,t)$ is to be chosen in such a way that the exact solution of the given problem is $t^\beta + e^s + s + 2$. The considered example is obtained from Equation 1 by applying the transformation $\tau = T - t$. The comparison of maximum absolute errors for different values of (α_1, α_2) is reported in Table 15. From the table, it can be seen that (α_1, α_2)=(1.5, 1.25) is the best case among all considered cases. Table 16 presents the maximum absolute errors of the proposed method by using

$k_1 = k_2 = 2$ and $M_1 = M_2 = 3$. In this table, we have compared the proposed method with the methods in [23] and [32], which shows the accuracy of the proposed method. Table 17 shows the maximum absolute errors, CR, and CPU time at $k_1 = 2$, $k_2 = 2$, $\alpha_1 = 1$, and $\alpha_2 = 0.5$. Figure 4 shows the plots of numerical and absolute error for (α_1, α_2)=(1.5,1.25) and $\beta = 0.5$.

Table 15: Comparison of maximum absolute error for Example 4 with $k_1 = k_2 = 2$, $M_1 = M_2 = 3$, $\beta = 0.5$

$\alpha_1 \backslash \alpha_2$		0.25	0.5	0.75	1	1.25	1.5
0.25	Method in [23]	$8.51 \cdot 10^{-3}$	$8.06 \cdot 10^{-6}$	$7.13 \cdot 10^{-14}$	$8.60 \cdot 10^{-12}$	$9.86 \cdot 10^{-12}$	$6.78 \cdot 10^{-11}$
	Proposed method	$2.34 \cdot 10^{-15}$	$1.36 \cdot 10^{-15}$	$1.61 \cdot 10^{-15}$	$1.77 \cdot 10^{-15}$	$1.57 \cdot 10^{-15}$	$5.58 \cdot 10^{-15}$
0.5	Method in [23]	$1.06 \cdot 10^{-12}$	$2.26 \cdot 10^{-5}$	$5.47 \cdot 10^{-12}$	$2.08 \cdot 10^{-13}$	$2.01 \cdot 10^{-13}$	$3.09 \cdot 10^{-13}$
	Proposed method	$8.34 \cdot 10^{-17}$	$1.87 \cdot 10^{-17}$	$4.07 \cdot 10^{-17}$	$4.95 \cdot 10^{-17}$	$3.20 \cdot 10^{-17}$	$3.96 \cdot 10^{-17}$
0.75	Method in [23]	$1.17 \cdot 10^{-2}$	$2.21 \cdot 10^{-4}$	$6.48 \cdot 10^{-15}$	$2.46 \cdot 10^{-16}$	$2.46 \cdot 10^{-16}$	$4.35 \cdot 10^{-16}$
	Proposed method	$1.01 \cdot 10^{-16}$	$4.62 \cdot 10^{-17}$	$4.59 \cdot 10^{-17}$	$4.77 \cdot 10^{-17}$	$2.87 \cdot 10^{-17}$	$5.00 \cdot 10^{-17}$
1	Method in [23]	$1.38 \cdot 10^{-15}$	$1.86 \cdot 10^{-16}$	$7.52 \cdot 10^{-15}$	$2.06 \cdot 10^{-16}$	$1.83 \cdot 10^{-16}$	$3.25 \cdot 10^{-16}$
	Proposed method	$4.61 \cdot 10^{-17}$	$2.25 \cdot 10^{-17}$	$6.23 \cdot 10^{-17}$	$2.12 \cdot 10^{-17}$	$2.58 \cdot 10^{-17}$	$3.09 \cdot 10^{-17}$
1.25	Method in [23]	$2.07 \cdot 10^{-15}$	$1.01 \cdot 10^{-8}$	$5.41 \cdot 10^{-14}$	$1.56 \cdot 10^{-16}$	$1.46 \cdot 10^{-16}$	$1.99 \cdot 10^{-16}$
	Proposed method	$3.73 \cdot 10^{-17}$	$3.10 \cdot 10^{-17}$	$4.69 \cdot 10^{-17}$	$1.57 \cdot 10^{-17}$	$3.23 \cdot 10^{-17}$	$3.63 \cdot 10^{-17}$
1.5	Method in [23]	$3.52 \cdot 10^{-2}$	$1.40 \cdot 10^{-16}$	$6.61 \cdot 10^{-3}$	$2.40 \cdot 10^{-16}$	$4.38 \cdot 10^{-16}$	$3.24 \cdot 10^{-16}$
	Proposed method	$2.13 \cdot 10^{-17}$	$3.99 \cdot 10^{-17}$	$3.30 \cdot 10^{-17}$	$2.10 \cdot 10^{-17}$	$1.15 \cdot 10^{-17}$	$3.16 \cdot 10^{-17}$

Table 16: Maximum absolute errors of Example 4 with $k_1 = k_2 = 2$, $M_1 = M_2 = 3$

β	Proposed method	Method in [23]	Method in [32]
0.1	$1.48 \cdot 10^{-17}$	$2.92 \cdot 10^{-16}$	$1.51 \cdot 10^{-5}$
0.3	$4.71 \cdot 10^{-17}$	$2.61 \cdot 10^{-16}$	$2.95 \cdot 10^{-5}$
0.5	$1.57 \cdot 10^{-17}$	$1.40 \cdot 10^{-16}$	$3.28 \cdot 10^{-5}$
0.7	$2.10 \cdot 10^{-17}$	$1.48 \cdot 10^{-16}$	$3.26 \cdot 10^{-5}$
0.9	$1.19 \cdot 10^{-17}$	$1.58 \cdot 10^{-16}$	$3.10 \cdot 10^{-5}$

Example 5. Consider the following non homogeneous time fractional BSE [23]:

$$\frac{\partial^\beta \mathscr{U}(s,t)}{\partial t^\beta} + \frac{1}{2}\sigma^2 s^2 \frac{\partial^2 \mathscr{U}(s,t)}{\partial s^2} + rs\frac{\partial \mathscr{U}(s,t)}{\partial s} - r\mathscr{U}(s,t) = 0, \tag{26}$$

with I.C and B.Cs

$$\begin{aligned} u &= e^{-(s-5)^2} \text{ on } \Omega_b = \{(s,1)|0.1 \le s \le 10\}, \\ u &= 0 \text{ on } \Omega_l = \{(0,t)|0 \le t \le 1\}, \\ u &= 0 \text{ on } \Omega_r = \{(1,t)|0 \le t \le 1\}. \end{aligned}$$

Here $r = 0.05, \sigma = 0.15$. $\mathscr{U}(s,1) = e^{-(s-5)^2}$ is a smooth payoff function. Following [23], we have taken $\beta = 0.7$. The exact solution of the above problem is unknown; therefore, to calculate the error, we use the following formula of residual error given as

$$\mathscr{R}_e(s,t) = \left| \frac{\partial^\beta \hat{\mathscr{U}}(s,t)}{\partial t^\beta} + \frac{1}{2}\sigma^2 s^2 \frac{\partial^2 \hat{\mathscr{U}}(s,t)}{\partial s^2} + rs\frac{\partial \hat{\mathscr{U}}(s,t)}{\partial s} - r\hat{\mathscr{U}}(s,t) \right|,$$

Table 17: Maximum absolute errors, CR, and CPU time at $k_1 = k_2 = 2$, $\alpha_1 = 1$, and $\alpha_2 = 0.5$ for Example 4

	$M_2 = 2$	$M_2 = 4$	$M_2 = 8$	$M_2 = 16$
$\beta = 0.5, M_1 = 2$	$1.14 \cdot 10^{-17}$	$4.17 \cdot 10^{-18}$	$3.12 \cdot 10^{-19}$	$5.12 \cdot 10^{-20}$
CR	–	1.450	3.74	2.60
CPU(s)	5.55	24.20	26.18	34.10
$\beta = 0.7, M_1 = 2$	$2.16 \cdot 10^{-17}$	$5.62 \cdot 10^{-18}$	$4.13 \cdot 10^{-19}$	$6.61 \cdot 10^{-20}$
CR	–	1.94	3.76	2.64
CPU(s)	5.66	25.82	24.66	37.22

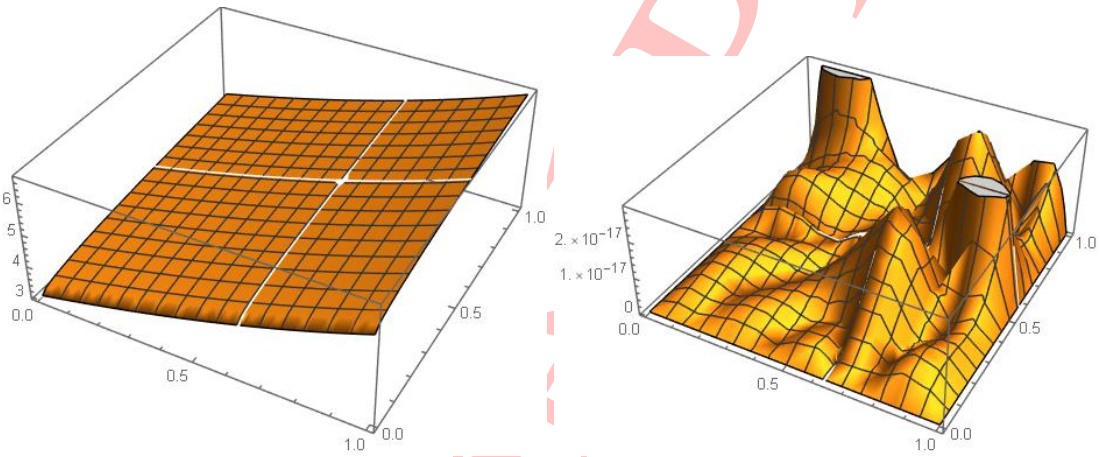

(a) **(b)**

Figure 4: (a) Plot of numerical solution using FOGCW with $k_1 = k_2 = 2$, $M_1 = M_2 = 3$, $\alpha_1 = 1.5, \alpha_2 = 1.25$, and $\beta = 0.5$, (b) plot of absolute errors using FOGCW with $k_1 = k_2 = 2$, $M_1 = M_2 = 3$, $\alpha_1 = 1.5, \alpha_2 = 1.25$, and $\beta = 0.5$ for Example 4

where $\hat{\mathscr{U}}(s,t)$ denotes the numerical solution. Table 18 shows the comparison of residual errors for different values of (α_1, α_2) with $k_1 = k_2 = M_1 = M_2 = 3$ and $\beta = 0.7$. From this table, we observe that $(\alpha_1, \alpha_2) = (1,1)$ is the best case among all considered cases. Table 19 shows the residual errors, CR, and CPU time at $k_1 = 3$, $k_2 = 3$, and $\alpha_1 = \alpha_2 = 1$. Figure 5 shows the plot of numerical solution for $(\alpha_1, \alpha_2) = (1,1)$, $\beta = 0.7$ and $k_1 = k_2 = 3$, $M_1 = M_2 = 4$. This figure confirms that the proposed method is accurate and highly effective in dealing with TFBSE with a smooth payoff function.

Example 6. Consider the following European type call option [32]:

$$\frac{\partial^{\beta} \mathscr{U}(s,t)}{\partial t^{\beta}} - \frac{1}{2}\sigma^2 s^2 \frac{\partial^2 \mathscr{U}(s,t)}{\partial s^2} - rs\frac{\partial \mathscr{U}(s,t)}{\partial s} + r\mathscr{U}(s,t) = 0, \ (s,t) \in (L,R) \times (0,T], \tag{26}$$

with I.C and B.Cs

$$\mathscr{U}(s,0) = \max(s-E,0), \ \ s \in (L,R),$$
$$\mathscr{U}(L,t) = 0, \ \ \mathscr{U}(R,t) = R - Ee^{-rt}, \ t \in (0,T],$$

Table 18: Comparison of residual errors at $k_1 = k_2 = M_1 = M_2 = 3$, and $\beta = 0.7$ for Example 5

(α_1, α_2) \ (s,t)		(1.0,0.1)	(3.0,0.3)	(5.0,0.5)	(7.0,0.7)	(9.0,0.9)
(0.5,0.5)	Method in [23]	$1.09 \cdot 10^{-3}$	$1.86 \cdot 10^{-2}$	$1.56 \cdot 10^{-1}$	$9.73 \cdot 10^{-2}$	$5.84 \cdot 10^{-3}$
	Proposed method	$1.45 \cdot 10^{-4}$	$3.60 \cdot 10^{-3}$	$6.12 \cdot 10^{-2}$	$1.14 \cdot 10^{-2}$	$5.94 \cdot 10^{-6}$
(1.0,1.0)	Method in [23]	$2.12 \cdot 10^{-3}$	$3.85 \cdot 10^{-3}$	$1.19 \cdot 10^{-2}$	$9.63 \cdot 10^{-2}$	$2.93 \cdot 10^{-3}$
	Proposed method	$5.57 \cdot 10^{-5}$	$3.33 \cdot 10^{-3}$	$5.92 \cdot 10^{-4}$	$1.00 \cdot 10^{-3}$	$5.94 \cdot 10^{-6}$
(1.5,1.5)	Method in [23]	$1.09 \cdot 10^{-3}$	$1.86 \cdot 10^{-2}$	$1.56 \cdot 10^{-1}$	$9.73 \cdot 10^{-2}$	$5.84 \cdot 10^{-3}$
	Proposed method	$1.45 \cdot 10^{-4}$	$3.60 \cdot 10^{-3}$	$6.12 \cdot 10^{-2}$	$1.14 \cdot 10^{-2}$	$5.94 \cdot 10^{-6}$
(0.5,1.0)	Method in [23]	$1.09 \cdot 10^{-3}$	$1.86 \cdot 10^{-2}$	$1.56 \cdot 10^{-1}$	$9.73 \cdot 10^{-2}$	$5.84 \cdot 10^{-3}$
	Proposed method	$1.45 \cdot 10^{-4}$	$3.60 \cdot 10^{-3}$	$6.12 \cdot 10^{-2}$	$1.14 \cdot 10^{-2}$	$5.94 \cdot 10^{-6}$
(1.0,0.5)	Method in [23]	$1.09 \cdot 10^{-3}$	$1.86 \cdot 10^{-2}$	$1.56 \cdot 10^{-1}$	$9.73 \cdot 10^{-2}$	$5.84 \cdot 10^{-3}$
	Proposed method	$1.45 \cdot 10^{-4}$	$3.60 \cdot 10^{-3}$	$6.12 \cdot 10^{-2}$	$1.14 \cdot 10^{-2}$	$5.94 \cdot 10^{-6}$
(1.5,1.0)	Method in [23]	$1.09 \cdot 10^{-3}$	$1.86 \cdot 10^{-2}$	$1.56 \cdot 10^{-1}$	$9.73 \cdot 10^{-2}$	$5.84 \cdot 10^{-3}$
	Proposed method	$1.45 \cdot 10^{-4}$	$3.60 \cdot 10^{-3}$	$6.12 \cdot 10^{-2}$	$1.14 \cdot 10^{-2}$	$5.94 \cdot 10^{-6}$
(1.0,1.5)	Method in [23]	$3.53 \cdot 10^{-3}$	$7.08 \cdot 10^{-3}$	$8.24 \cdot 10^{-2}$	$9.76 \cdot 10^{-2}$	$2.94 \cdot 10^{-3}$
	Proposed method	$1.27 \cdot 10^{-4}$	$3.63 \cdot 10^{-3}$	$1.90 \cdot 10^{-2}$	$1.23 \cdot 10^{-2}$	$1.24 \cdot 10^{-5}$

Table 19: Residual errors, CR, and CPU time at $k_1 = 3$, $k_2 = 3$, $\alpha_1 = \alpha_2 = 1$ for Example 5

	$M_2 = 2$	$M_2 = 4$	$M_2 = 8$	$M_2 = 16$
$\beta = 0.5, M_1 = 4$	$3.23 \cdot 10^{-3}$	$2.67 \cdot 10^{-4}$	$1.66 \cdot 10^{-5}$	$1.32 \cdot 10^{-6}$
CR	–	3.59	2.77	3.65
CPU(s)	7.09	23.16	35.28	49.10
$\beta = 0.7, M_1 = 4$	$1.23 \cdot 10^{-3}$	$2.66 \cdot 10^{-4}$	$6.23 \cdot 10^{-5}$	$1.12 \cdot 10^{-6}$
CR	–	2.20	2.09	5.79
CPU(s)	7.66	24.12	35.66	41.22

with parameters $\sigma = 0.3$, $r = 0.04$, $E = 10$, $T = 1$, $L = 0$, $R = 40$, and E denotes the exercise price. The considered example is obtained from Equation 1 by applying the transformation $\tau = T - t$.
The exact solution of this problem is not known. Therefore, the double mesh principle is used to estimate the errors. Clearly, the given problem has a non-smooth payoff. To solve the above problem by the proposed method, we first transform the non-smooth payoff with a smooth payoff $\mathscr{U}(s,T) = \xi(s-E)$, where $\xi(s)$ [38] is a function given by

$$\xi(s) = \begin{cases} s, & s \geq -\varepsilon, \\ a_0 + a_1 s + a_2 s^2 + \cdots + a_9 s^9, & -\varepsilon < s < \varepsilon, \\ 0, & s \leq \varepsilon, \end{cases}$$

where $a_0 = \frac{35\varepsilon}{256}$, $a_1 = \frac{1}{2}$, $a_2 = \frac{35}{64\varepsilon}$, $a_3 = 0$, $a_4 = \frac{-35}{128\varepsilon}$, $a_5 = 0$, $a_6 = \frac{7}{64\varepsilon^3}$, $a_7 = 0$, $a_8 = \frac{-5}{256\varepsilon^7}$, $a_9 = 0$ for $\varepsilon > 0$. Table 20 compares the maximum absolute errors and convergence rate in space with the

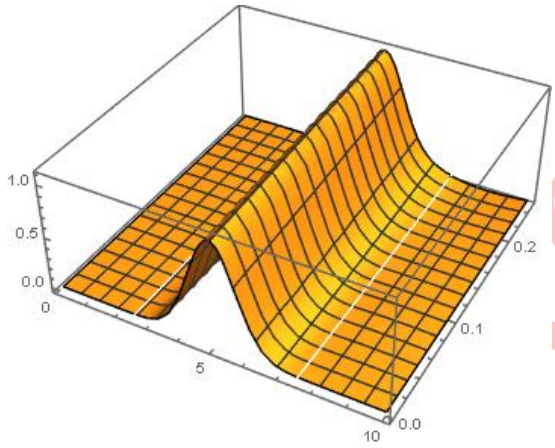

Figure 5: Plot of numerical solution using FOGCW with $k_1 = k_2 = 3$, $M_1 = M_2 = 4$, $\alpha_1 = \alpha_2 = 1$, and $\beta = 0.7$ for Example 5

method in [33] for different values of β with $\varepsilon = 10$, $\sigma = 0.25$, $r = 0.05$, $E = 50$, and $T = 1$. From the table, we can see that by taking lower values of M_1, the proposed wavelet-based method achieves good convergence and maintains acceptable accuracy. Table 21 compares the maximum absolute errors and convergence rate in time with the method in [32] for different values of β with $\varepsilon = 5$, $\sigma = 0.3$, $r = 0.04$, $E = 10$, and $T = 1$. Clearly, a smaller error and high convergence rate are achieved in our case by using small values of M_2. Figure 6 shows the approximate plot and error plot for $k_1 = k_2 = 1$, $M_1 = M_2 = 2$, $\alpha_1 = \alpha_2 = 1$, and $\beta = 0.99$.

Table 20: Comparison of maximum absolute errors, CR at $k_1 = k_2 = 1$, $\alpha_1 = \alpha_2 = 1$ for Example 6

β	Proposed method ($M_2 = 2$)			Method in [33] ($M_2 = 100$)				
	M_1	$\mathscr{E}_\infty$	CR	M_1	$\mathscr{E}_\infty$ by L-12	CR	$\mathscr{E}_\infty$ by $L2$-1_σ	CR
0.89	2	$3.42 \cdot 10^{-2}$	–	32	$1.90 \cdot 10^{-2}$	–	$1.91 \cdot 10^{-2}$	–
	4	$1.51 \cdot 10^{-2}$	1.17	64	$1.38 \cdot 10^{-2}$	0.47	$1.38 \cdot 10^{-2}$	0.47
	8	$1.01 \cdot 10^{-3}$	3.90	128	$9.45 \cdot 10^{-4}$	3.86	$9.45 \cdot 10^{-4}$	3.87
	16	$8.51 \cdot 10^{-5}$	6.29	256	$5.81 \cdot 10^{-5}$	4.02	$5.80 \cdot 10^{-5}$	4.03
0.94	2	$2.06 \cdot 10^{-2}$	–	32	$1.99 \cdot 10^{-2}$	–	$1.99 \cdot 10^{-2}$	–
	4	$8.43 \cdot 10^{-3}$	1.28	64	$1.51 \cdot 10^{-2}$	0.47	$1.51 \cdot 10^{-2}$	0.40
	8	$1.22 \cdot 10^{-4}$	4.23	128	$1.00 \cdot 10^{-3}$	3.86	$1.00 \cdot 10^{-3}$	3.92
	16	$1.36 \cdot 10^{-6}$	6.48	256	$6.50 \cdot 10^{-5}$	4.02	$6.50 \cdot 10^{-5}$	3.94
0.99	2	$6.54 \cdot 10^{-3}$	–	32	$2.07 \cdot 10^{-2}$	–	$2.07 \cdot 10^{-2}$	–
	4	$1.44 \cdot 10^{-3}$	1.17	64	$1.66 \cdot 10^{-2}$	0.32	$1.65 \cdot 10^{-2}$	0.32
	8	$1.08 \cdot 10^{-4}$	3.90	128	$1.04 \cdot 10^{-3}$	3.99	$1.04 \cdot 10^{-3}$	3.99
	16	$3.12 \cdot 10^{-6}$	6.29	256	$7.65 \cdot 10^{-5}$	3.76	$7.65 \cdot 10^{-5}$	3.76

Table 21: Comparison of maximum absolute errors, CR at $k_1 = k_2 = 1$, $\alpha_1 = \alpha_2 = 1$ for Example 6

β	Proposed method ($M_1 = 2$)			Method in [32] ($M_1 = 1024$)		
	M_2	$\mathscr{E}_\infty$	CR	M_2	$\mathscr{E}_\infty$	CR
0.1	2	$1.96 \cdot 10^{-1}$	–	64	$2.03 \cdot 10^{-1}$	–
	4	$1.06 \cdot 10^{-1}$	0.88	128	$1.24 \cdot 10^{-1}$	0.70
	8	$2.60 \cdot 10^{-2}$	2.02	256	$7.35 \cdot 10^{-2}$	0.76
	16	$4.23 \cdot 10^{-4}$	7.28	512	$4.21 \cdot 10^{-2}$	0.80
0.3	2	$1.78 \cdot 10^{-1}$	–	64	$2.15 \cdot 10^{-1}$	–
	4	$9.93 \cdot 10^{-2}$	0.84	128	$1.17 \cdot 10^{-1}$	0.87
	8	$4.38 \cdot 10^{-2}$	1.18	256	$6.26 \cdot 10^{-2}$	0.90
	16	$4.23 \cdot 10^{-4}$	6.69	512	$3.29 \cdot 10^{-2}$	0.92
0.5	2	$1.01 \cdot 10^{-1}$	–	64	$1.93 \cdot 10^{-1}$	–
	4	$5.55 \cdot 10^{-2}$	0.86	128	$1.00 \cdot 10^{-1}$	0.95
	8	$1.28 \cdot 10^{-2}$	2.11	256	$5.11 \cdot 10^{-2}$	0.96
	16	$5.81 \cdot 10^{-3}$	4.94	512	$2.591 \cdot 10^{-2}$	0.97
0.7	2	$5.13 \cdot 10^{-2}$	–	64	$1.83 \cdot 10^{-1}$	–
	4	$2.44 \cdot 10^{-2}$	1.07	128	$9.44 \cdot 10^{-2}$	0.95
	8	$7.72 \cdot 10^{-3}$	1.66	256	$4.83 \cdot 10^{-2}$	0.96
	16	$7.38 \cdot 10^{-6}$	10.03	512	$2.44 \cdot 10^{-2}$	0.98
0.9	2	$1.96 \cdot 10^{-1}$	–	64	$2.10 \cdot 10^{-1}$	–
	4	$1.06 \cdot 10^{-1}$	0.88	128	$1.06 \cdot 10^{-1}$	0.97
	8	$2.60 \cdot 10^{-2}$	2.02	256	$5.38 \cdot 10^{-2}$	0.98
	16	$4.23 \cdot 10^{-4}$	7.28	512	$2.70 \cdot 10^{-2}$	0.99

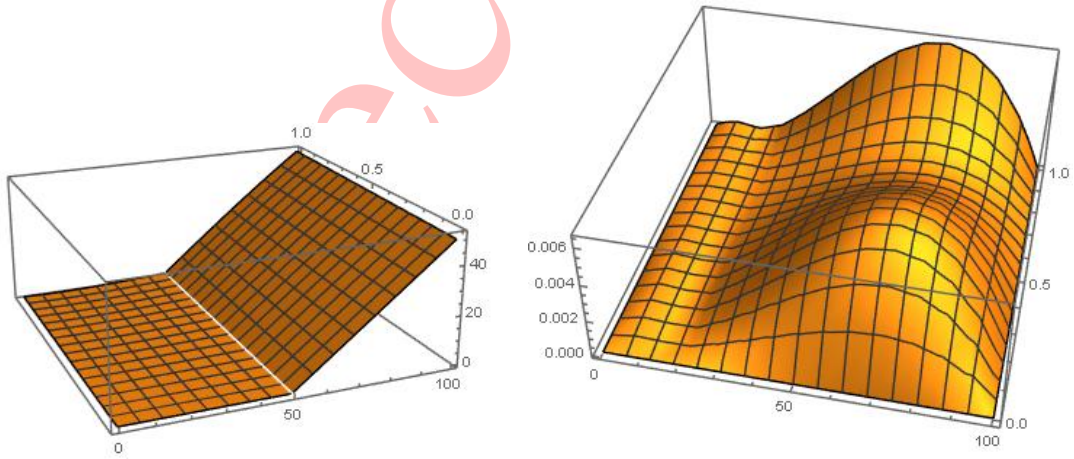

(a) **(b)**

Figure 6: (a) Plot of numerical solution using FOGCW with $k_1 = k_2 = 1$, $M_1 = M_2 = 2$, $\alpha_1 = \alpha_2 = 1$, and $\beta = 0.99$, (b) plot of absolute errors using FOGCW with $k_1 = k_2 = 1$, $M_1 = M_2 = 2$, $\alpha_1 = \alpha_2 = 1$, and $\beta = 0.99$ for Example 6

7 Conclusion

This study successfully presented a novel numerical method for solving the time-fractional Black-Scholes equation (TFBSE) using a fractional-order generalized Chelyshkov wavelet (FOGCW) coupled with the collocation technique. Several inherent properties of the FOGCW provide a robust mathematical foundation; specifically, deriving an exact formula for the Riemann-Liouville fractional integral operator using the regularized beta function is the key point of the present method. To test the computational efficacy and accuracy of the proposed method, several numerical examples are demonstrated. For Examples 1–6, we have compared the proposed method with the other existing methods, showing the robustness of the proposed method. In Example 5, we have taken TFBSE, whose exact solution is not known, so we have used the concept of residual error to calculate the absolute error. We have considered European call option with a non-smooth payoff as Example 6, which reflects realistic market conditions. The proposed method successfully solved the European option with a smooth payoff as well as a non-smooth payoff function, which validates the method's practicability. The proposed framework is highly adaptable and well suited for solving fractional option pricing problems arising in real financial markets. Future direction is to extend the proposed framework to solve higher-dimensional and distributed order fractional BSE.

References

[1] F. Black, M. Scholes, *The pricing of options and corporate liabilities*, J. Polit. Econ. **81(3)** (1973) 637–654.

[2] R. Gorenflo, F. Mainardi, E. Scalas, M. Raberto, *Fractional calculus and continuous-time finance III: the diffusion limit*, in: Mathematical Finance, Springer, 2001, 171–180.

[3] F. Mainardi, M. Raberto, R. Gorenflo, E. Scalas, *Fractional calculus and continuous-time finance II: the waiting-time distribution*, Phys. A **287(3-4)** (2000) 468–481.

[4] J. Mohapatra, S. Mohapatra, A. Nath, *An approximation technique for a system of time-fractional differential equations arising in population dynamics*, J. Math. Model. **13(3)** (2025) 519–531.

[5] P. Carr, L. Wu, *The finite moment log stable process and option pricing*, J. Finance **58(2)** (2003) 753–777.

[6] S.A. David, J.T. Machado, L.R. Trevisan, C.M. Inácio Jr, A.M. Lopes, *Dynamics of commodities prices: integer and fractional models*, Fundam. Inform. **151(1-4)** (2017) 389–408.

[7] W. Wyss, *The fractional Black–Scholes equation*, Fract. Calc. Appl. Anal. **3** (2000) 51–61.

[8] A. Cartea, D. del Castillo-Negrete, *Fractional diffusion models of option prices in markets with jumps*, Phys. A **374(2)** (2007) 749–763.

[9] J.R. Liang, J. Wang, W.J. Zhang, W.Y. Qiu, F.Y. Ren, *Option pricing of a bi-fractional Black–Merton–Scholes model with the Hurst exponent H in* $[\frac{1}{2}, 1]$, Appl. Math. Lett. **23(8)** (2010) 859–863.

[10] W. Chen, X. Xu, S.P. Zhu, *Analytically pricing double barrier options based on a time-fractional Black–Scholes equation*, Comput. Math. Appl. **69(12)** (2015) 1407–1419.

[11] M. She, L. Li, R. Tang, D. Li, *A novel numerical scheme for a time fractional Black–Scholes equation*, J. Appl. Math. Comput. **66(1)** (2021) 853–870.

[12] S. Ampun, P. Sawangtong, *The Approximate analytic solution of the time-fractional Black–Scholes equation with a European option based on the Katugampola fractional derivative*, Mathematics **9(3)** (2021) 214.

[13] K. Kazmi, *A second order numerical method for the time-fractional Black–Scholes European option pricing model*, J. Comput. Appl. Math. **418** (2023) 114647.

[14] P. Roul, V.P. Goura, *A compact finite difference scheme for fractional Black–Scholes option pricing model*, Appl. Numer. Math. **166** (2021) 40–60.

[15] A. Atta, M. Abdelkawy, A. Napoli, W. Abd-Elhameed, *Galerkin approach by certain shifted Jacobi polynomials for solving the time-fractional Black–Scholes equation*, Bound. Value Probl. **2025(1)** (2025) 138.

[16] Y. Li, W. Zhao, *Haar wavelet operational matrix of fractional order integration and its applications in solving the fractional order differential equations*, Appl. Math. Comput. **216(8)** (2010) 2276–2285.

[17] Z. Barikbin, E. Keshavarz, *Solving fractional optimal control problems by new Bernoulli wavelets operational matrices*, Optim. Control Appl. Methods **41(4)** (2020) 1188–1210.

[18] M.H. Heydari, M. Razzaghi, *A numerical approach for a class of nonlinear optimal control problems with piecewise fractional derivative*, Chaos Solit. Fractals **152** (2021) 111465.

[19] M.H. Heydari, Z. Avazzadeh, *A new wavelet method for variable-order fractional optimal control problems*, Asian J. Control **20(5)** (2018) 1804–1817.

[20] G. Dewangan, A. Singh, A. Kanaujiya, *Generalized distributed-order fractional optimal control problem using Laguerre wavelet method*, J. Math. Model. **13(4)** (2025) 747–765.

[21] S. Mashayekhi, M. Razzaghi, *Numerical solution of distributed order fractional differential equations by hybrid functions*, J. Comput. Phys. **315** (2016) 169–181.

[22] P. Vichitkunakorn, T.N. Vo, M. Razzaghi, *A numerical method for fractional pantograph differential equations based on Taylor wavelets*, Trans. Inst. Meas. Control **42(7)** (2020) 1334–1344.

[23] B. Yuttanan, M. Razzaghi, T.N. Vo, *An Efficient wavelet method for time-fractional Black–Scholes equations*, Math. Methods Appl. Sci. **47(15)** (2024) 12321–12339.

[24] H. Zhang, F. Liu, I. Turner, Q. Yang, *Numerical solution of the time fractional Black–Scholes model governing European options*, Comput. Math. Appl. **71(9)** (2016) 1772–1783.

[25] R.H. De Staelen, A.S. Hendy, *Numerically pricing double barrier options in a time-fractional Black–Scholes model*, Comput. Math. Appl. **74(6)** (2017) 1166–1175.

[26] A. Golbabai, O. Nikan, *A computational method based on the moving least-squares approach for pricing double barrier options in a time-fractional Black–Scholes model*, Comput. Econ. **55(1)** (2020) 119–141.

[27] H. Mesgarani, S. Ahanj, Y. Esmaeelzade Aghdam, *Numerical investigation of the time-fractional Black-Scholes equation with barrier choice of regulating European option*, J. Math. Model. **10(1)** (2022) 1–10.

[28] N. Abdi, H. Aminikhah, A.R. Sheikhani, *High-order compact finite difference schemes for the time-fractional Black-Scholes model governing European options*, Chaos Solit. Fractals **162** (2022) 112423.

[29] M. Taghipour, H. Aminikhah, *A spectral collocation method based on fractional pell functions for solving time–fractional Black–Scholes option pricing model*, Chaos Solit. Fractals **163** (2022) 112571.

[30] P. Roul, *A high accuracy numerical method and its convergence for time-fractional Black-Scholes equation governing European options*, Appl. Numer. Math. **151** (2020) 472–493.

[31] A. Golbabai, O. Nikan, T. Nikazad, *Numerical analysis of time fractional Black–Scholes European option pricing model arising in financial market*, Comput. Appl. Math. **38(4)** (2019) 173.

[32] Z. Cen, J. Huang, A. Xu, A. Le, *Numerical approximation of a time-fractional Black–Scholes equation*, Comput. Math. Appl. **75(8)** (2018) 2874–2887.

[33] S. Tarei, A. Kanaujiya, J. Mohapatra, *Efficient numerical method for pricing option with underlying asset follows a fractal stochastic process*, Comput. Methods Differ. Equ. (2025) 1–27.

[34] J. Kaur, S. Natesan, *A novel numerical scheme for time-fractional Black-Scholes pde governing European options in mathematical finance*, Numer. Algorithms **94(4)** (2023) 1519–1549.

[35] P. Yadav, S. Jahan, K.S. Nisar, *Fibonacci wavelet method for time fractional convection–diffusion equations*, Math. Methods Appl. Sci. **47(4)** (2024) 2639–2655.

[36] H.T. Ngo, M. Razzaghi, T.N. Vo, *Fractional-order Chelyshkov wavelet method for solving variable-order fractional differential equations and an application in variable-order fractional relaxation system*, Numer. Algorithms **92(3)** (2023) 1571–1588.

[37] P. Rahimkhani, Y. Ordokhani, P. Lima, *An improved composite collocation method for distributed-order fractional differential equations based on fractional Chelyshkov wavelets*, Appl. Numer. Math. **145** (2019) 1–27.

[38] S.C.S. Rao, Manisha, *Numerical solution of generalized Black–Scholes model*, Appl. Math. Comput. **321** (2018) 401–421.

[39] F. Zakipour, A. Saadatmandi, *A novel fractional Bernoulli–Picard iteration method to solve fractional differential equations*, J. Math. Model. **13(1)** (2025) 139–152.

[40] S. Zerbib, K. Hilal, A. Kajouni, *Nonlocal Caputo generalized proportional fractional integro-differential systems: an existence study*, J. Math. Model. **13(2)** (2025) 375–391.